Waste and Biomass Valorization (2022) 13:4749–4770
https://doi.org/10.1007/s12649-022-01800-2

ORIGINAL PAPER

Integrated CO_2 Capture and Nutrient Removal by Microalgae *Chlorella vulgaris* and Optimization Using Neural Network and Support Vector Regression

Nima Hajinajaf[1] · Alireza Fallahi[1] · Yahya Rabbani[1] · Omid Tavakoli[1] · Mohammad-Hossein Sarrafzadeh[1]

Received: 1 December 2021 / Accepted: 1 May 2022 / Published online: 3 June 2022

Abstract

Microalgae are useful for the mitigation of carbon from point source CO_2 emission flue gases. The main aim of this work was to maximize the growth of microalgae *Chlorella vulgaris* in a pilot scale photobioreactor as well as CO_2 and nutrient removal. *Chlorella vulgaris* was cultured in three bubble column photobioreactors with the working volumes of 4, 9.6 and 16 L and CO_2 concentration of power plant flue gas (ranging from 0.04 to 15%), flow rate from 50 to 150 mL min^{-1} and the diameter of the photobioreactors were considered as study parameters. Optimal condition observed was for the reactor with the diameter of 10.5 cm, CO_2 concentration of 7.5% and flowrate of 100 mL min^{-1} with the maximum cell concentration and average CO_2 removal of 3.63 g. L^{-1} and 91.7%, respectively. Besides, total phosphorus removal of 100% and total nitrogen removal efficiency in the range of 81.5–94.1% observed for all the experiments which demonstrated a desirable design of bioreactors with high mixing efficiency. Finally, the effects of different studied parameters on the biomass concentration were predicted by Artificial Neural Network (ANN) and Support Vector Regression (SVR) methods. The Levenberg–Marquardt algorithm and Gaussian kernel with correlation coefficient values of 0.9937 and 0.9964 were selected as the optimal network.

Graphical Abstract

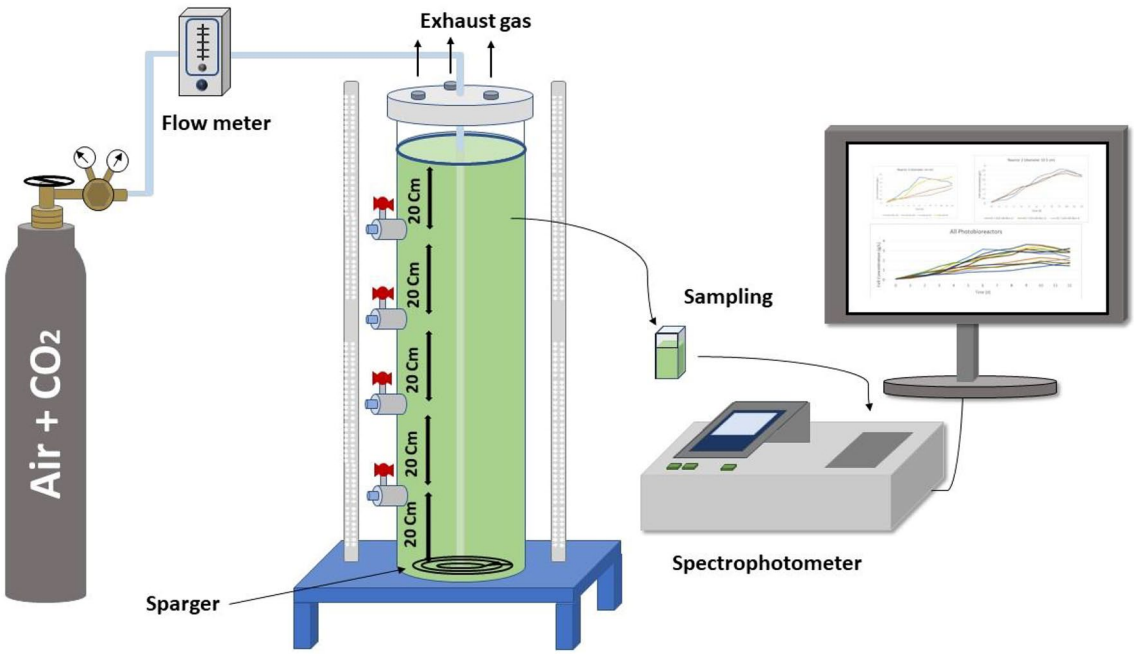

Extended author information available on the last page of the article

Keywords Photobioreactor · CO_2 removal · *Chlorella vulgaris* · Microalgae cultivation · Neural network · SVR

Statement of Novelty

The specific objective of this research was to investigate the impact of proper design and mixing efficiency of a bubble column photobioreactor on the microalgal biomass production, CO_2 biofixation and nutrient removal in pilot scale. To better simulate the real industrial scenario of CO_2 mitigation from power plants, CO_2 concentrations in the range of flue gas (0.04–15%), light intensity at the saturation point of *C. vulgaris* (~ 12,000 lx or 165 µmol m^{-2} s^{-1}) and a medium with higher concentrations of nitrate and phosphate compared to wastewater was considered. Besides, support vector regression and artificial neural network were used for microalgae growth optimization. The information provided in this research, shows that high microalgal biomass growth, CO_2 mitigation and nutrient removal is possible in a large scale system, if proper mixing and well-design are employed.

Introduction

Increasing carbon dioxide (CO_2) emissions in the atmosphere due to industrialization and burning of fossil fuels have caused numerous environmental problems. The amount of carbon dioxide in the atmosphere has reached 419.28 ppm in March 2022, with the growth of 8.24 ppm since March 2019 [1]. Various industries contribute to the global warming by exhausting CO_2 to the atmosphere with various compositions: coal fired power plants (12–14%), gas turbines (3–4%), blast furnace gas (27%), and natural gas fired boiler (7–10%) [2–4]. CO_2 emitted from these industries are either from a transporter sector (line source) or an industrial sector (point source) [5].

Many attempts have been made for Carbon Capture and Storage (CCS) in the past century [6]. CO_2 mitigation strategies are classified into three categories: chemical [7, 8], physical [9] and biological [10, 11]. Among these techniques, biological carbon capture using microorganisms has gained a lot of attention in recent years [12]. Besides that, pollutants and nutrient concentration have been increased in water systems, which impact human health as well as creating critical challenges for the environment and may lead to eutrophication [13–16]. Thus, it is necessary to decrease the nutrient content, especially nitrogen (N) and phosphorus (P), in the wastewater and control the pollutant discharge from wastewater treatment facilities [17]. Conventional wastewater treatment technologies currently apply anaerobic digestion and aerobic activated sludge which are unable to remove some of the nutrients (nitrogen and phosphorous) from wastewater efficiently [18] and thus advanced treatments are required to meet the discharge regulations.

Microalgae, as a fast-growing microorganism have the ability to fix CO_2 and microalgal biomass can be further used in pharmaceutical, food and other industries. Microalgae can also be regarded as a promising strategy for CO_2 mitigation since they can grow faster than terrestrial plants, tolerate extreme environments and can be easily incorporated into engineered systems [19]. Microalgae can be useful for the mitigation of carbon from point source CO_2 emission flue gases and simultaneously treat wastewater by uptaking nitrogen and phosphorous as nutrients [12, 20–22]. Microalgae cultivation in wastewater has gotten a lot of attention recently since it may help offset the capital costs of biomass production systems while wastewater can provide nutrients for microalgal growth. [12, 23].

Numerous studies have investigated the effects of CO_2 supply and light intensity on microalgal growth, biofixation efficiency, and nutrient removal [24–27]. Liu et al. [28], evaluated the influence of CO_2 concentration from 1 to 20% on *Chlorella vulgaris* (*C. vulgaris*) in domestic wastewater. Anjos et al. [20, 29], assessed the growth of *C.vulgaris* P12 using CO_2 concentrations of 2–10% and flow rates of 0.1–0.7 vvm in a bubble column photobioreactor. The biofixation efficiency of *Synechococcus elongatus* in hollow fiber membrane-sparger (MS-PBR) and contactor (MC-PBR) photobioreactors in CO_2 concentrations of 0.04%, 5% and 10% was accomplished by Mortezaeikia et al. [30]. Gonçalves et al. [31], investigated the effects of light irradiance and light/dark cycles on four different strains of microalgae for the aim of CO_2 and nutrient removal as well as biomass productivity. Although various research focused on improving the biomass productivity or nutrient removal from wastewater, the overall efficiency of these systems was not helpful to make the process economically viable and hence, microalgal growth as well as CO_2 and nutrient uptake efficiency need to be improved to overcome full-scale operation [10, 32].

In order to maximize the biofixation of CO_2 from flue gas, a suitable strain of microalgae with a high capacity to absorb CO_2 and a high tolerance to CO_2 concentrations should be selected [33–35]. Microalgae *chlorella vulgaris* have shown to have such capability [36–38] and therefore selected for this study. Moreover, bubble column photobioreactors demonstrated a viable technology for algal cultivation due to their low energy consumption, low shear stress, ease of operation, and low capital cost [33] allowing them to be selected and employed for full-scale microalgal production operations. However, in order to achieve the highest yield,

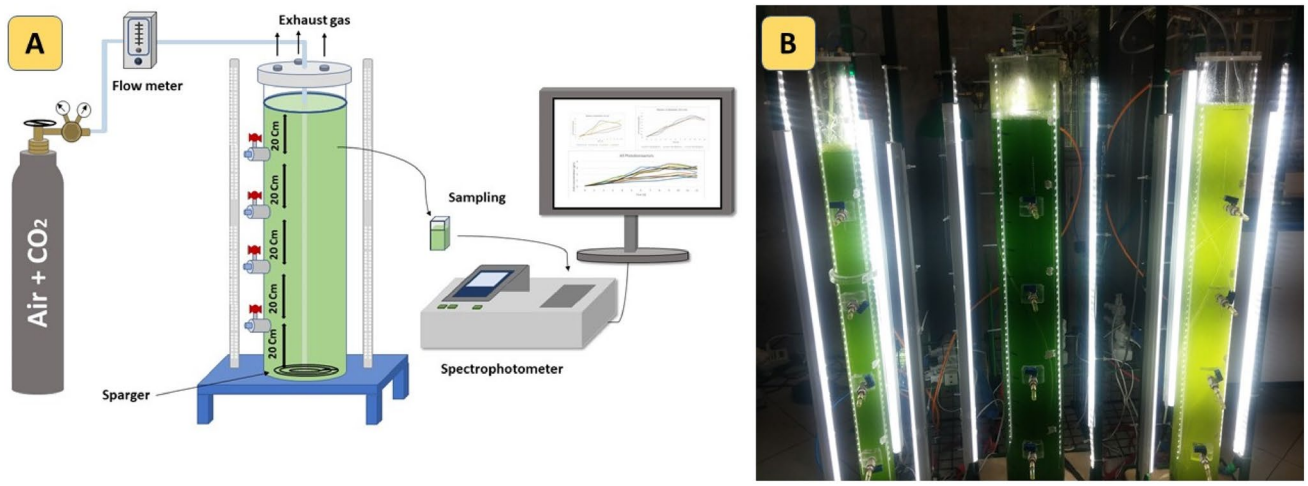

Fig. 1 Experimental system for the effects of CO_2, flow rate and column diameter on biomass growth, CO_2 removal and nutrient uptake, **a** schematic of the experimental setup, **b** image of the experimental PBRs

the best growth conditions for biomass, such as light intensity, CO_2 gas composition, flowrate, and photobioreactor geometry, must be practically determined. [29, 39].

While some published research has shown the effect of CO_2 concentration and light intensity on microalgal growth and CO_2 removal performance, considerable challenges remain, including understanding microalgae performance at the pilot size. Indeed, the vast majority of earlier research were conducted at the bench scale, which cannot be utilized correctly for pilot scale and full-scale operations. Furthermore, several studies have failed to explain the concurrent effect of operational factors such as CO_2 concentration and flow rate, as well as photobioreactor diameter, on nutrient removal, biomass growth, and CO_2 mitigation. Therefore, the objective of this study was to develop an experimental and modeling approach (by artificial neural network and support vector regression) to analyze the effect of the above-mentioned parameters on the performance of microalgae *C. vulgaris* cultivated in three pilot scale bubble column PBRs with the working volumes of 4, 9.6, and 16 L. In order to consider the real scenario of the work to be applicable in large scale cultivation, CO_2 concentrations in the range of flue gas (0.04–15% [40]) and light intensity at the saturation point of *C. vulgaris* [41] were considered.

Materials and Methods

Microorganisms and Culture Medium

The microalgae *Chlorella vulgaris* were purchased from Iranian Biological Resource Center (IBRC), Tehran, Iran. The strain was cultured in the BG-11 medium with the initial cell concentration of 0.1 g L^{-1}. The composition of BG-11 medium is as follows: $NaNO_3$ (1.5 g L^{-1}), K_2HPO_4 (0.04 g L^{-1}), $MgSO_4.7H_2O$ (0.075 g L^{-1}), Na_2CO_3 (0.02 g L^{-1}), citric acid (0.006 g L^{-1}), Ferric ammonium citrate (0.006 g L^{-1}), Na EDTA (0.001 g L^{-1}), H_3BO_3 (0.00286 g L^{-1}), $MnCl_2.2H_2O$ (0.00181 g L^{-1}), $ZnSO_4$ (0.000222 g L^{-1}), $CuSO_4.5H_2O$ (0.000079 g L^{-1}), $Na_2MoO_4.2H_2O$ (0.000390 g L^{-1}) and $Co(NO_3)_2.6H_2O$ (0.000049 g L^{-1}). All chemicals and media were purchased from Merck (Shanghai) and Ciba Co. Ltd. (Switzerland).

Experimental Set-Up

Three bubble column photobioreactors (PBRs) were constructed using 4 mm thickness Plexiglass, 110 cm in height and the diameters of 7, 10.5 and 14 cm (most available sizes of Plexiglass tubes in the market) with the approximate working volumes of 4, 9.6 and 16 L, respectively (From now, we name the reactors based on their diameters: PBR 1: 7 cm, PBR 2: 10.5 cm, and PBR 3: 14 cm). Three stands were made for each PBR to aid for easy discharge of culture as wells as cleaning and installing LEDs. One air pump and two CO_2 mixtures of 7.52% and 15% CO_2 + air cylinders were also provided as CO_2 source. Also, three spiral shape spargers were used as gas distributer at the bottom of each column. Three rotameters (Dwyer, USA) were installed to set and control the desired air flowrate. Experiments were carried out at 25 ± 2 °C and batch mode under 165 µmol m^{-2} s^{-1} of cool white fluorescent lamps with the light/dark cycles of 14/10 h. Measurement of the incident light intensity on the surface of the culture medium was also carried out using quantum meter (MQ-300 Apogee instruments, USA) and a spherical micro quantum sensor with a 3.7 mm diffusing sphere (WALZ US-SQS/L, USA) was utilized to accurately measure the light intensity at different

Table 1 Full factorial experimental design

Runs	CO_2 concentration %	Flow rate (mL/min)	Reactor diameter (cm)
1	15.00	150	14
2	15.00	150	7
3	0.04	150	14
4	7.52	100	10.5
5	0.04	50	14
6	7.52	100	10.5
7	0.04	50	7
8	15.00	50	7
9	7.52	100	10.5
10	0.04	150	7
11	15.00	50	14

distances from the surface of the photobioreactors. The schematic diagram and experimental setup of this study is shown in Fig. 1a and 1b, respectively.

Performance Assessment

Determination of Microalgal Cell Concentration

Biomass concentration was calculated daily by measuring the optical density of *C. vulgaris* at 680 nm wavelength using a UV-spectrophotometer (Vis 2100 Unico China/USA). Samples were taken from five sampling points of each photobioreactor at different heights of 20, 40, 60, 80, and 100 cm due to microalgal sedimentation along the column height, and the average daily data was represented. Cell concentration (g L^{-1}) was calculated by using calibration curve of absorbance and dried cell weight (DCW) of microalgal biomass ($R^2 > 0.98$), in which the DCW was measured by taking 5 mL of microalgal culture, being washed twice to remove the salts, and keeping in an oven overnight at 60 °C and calculated from Eq. (1):

$$\mathrm{DCW} = \mathrm{W}_2 - \mathrm{W}_1 \tag{1}$$

where W_1 is the weight of fresh foil paper, W_2 is the weight of foil paper and 5 mL of microalgal culture after drying. pH and temperature were determined using a pH meter (HANNA HI207 pH meter) daily.

Determination of Biomass Productivity and Specific Growth Rate

Biomass productivity (g L^{-1} d^{-1}) was calculated from changes in biomass concentration (g L^{-1}) over time (d) from Eq. (2):

$$P = \frac{X_2 - X_1}{t_2 - t_1} \tag{2}$$

where P signifies the biomass productivity, X_2 is cell concentration at time t_2 and X_1 is cell concentration at time t_1, and t_2–t_1 is the period of the growth phase.

Specific growth rate (d^{-1}) was also calculated from Eq. (3):

$$\mu = \frac{Ln\left(X_2/X_1\right)}{t_2 - t_1} \tag{3}$$

where X_2 and X_1 are cell concentrations at times t_2 and t_1, respectively.

Determination of Maximal CO_2 Fixation Rate

In order to measure the CO_2 removal efficiency, Eq. (4) has been used [42]:

$$\mathrm{CO_2 removal\ efficiency\%} = \left(1 - \frac{\mathrm{CO_2 output}}{\mathrm{CO_2 input}}\right) \times 100 \tag{4}$$

To measure the CO_2 output, samples were taken and analyzed by GC–MS.

Determination of Nitrogen and Phosphorus Removal Efficiency

The amounts of NO_3^--N and PO_4^{-3}-P were determined using the spectrophotometric standard method for the examination of water and wastewater [19, 43]. In order to measure the nitrate and phosphate content in the culture, 15 mL of culture medium were taken from the PBR and centrifuged at 5000 rpm for 15 min and filtered to prevent the availability of cells in the supernatant. 1 mL HCl 1 N was added to 5 mL of the filtered sample, mixed thoroughly, and its absorbance was read at the optical density (OD) = 220 nm and OD = 275 nm. In order to measure the nitrate concentration of the liquid, calibration curve was used. Amount of phosphate was also measured by the addition of 0.2 mL

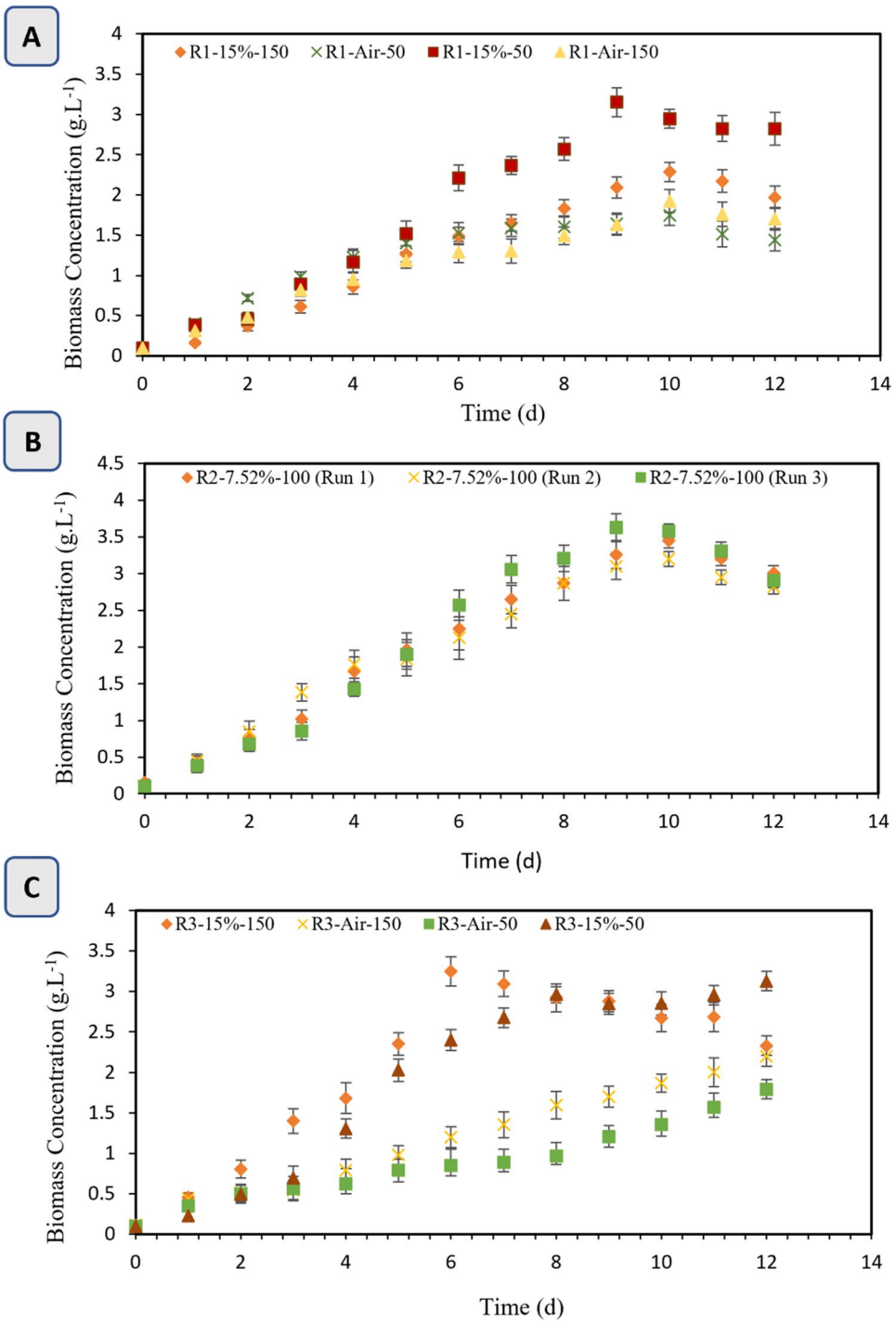

Fig. 2 Biomass concentration of C. *vulgaris* in PBRs 1, 2 and 3 during the cultivation period, **A** PBR1, **B** PBR2, **C** PBR3

of ammonium molybdate ($(NH_4)_6Mo_7O_{24}$) to the 5 mL of the filtered sample and mixed with 20 µL stannous chloride ($SnCl_2$) solution. Finally, its optical density was read at 650 nm after 8 min and the phosphate content was obtained from the calibration curve.

Experimental Design and Analysis

Maximum CO_2 composition of the power plant flue gas (ranging from 5 to 15%) was considered as the maximum CO_2 concentration [44]. After construction of three

photobioreactors with different diameters and by assuming the constant solar radiation, an equivalent light intensity of 165 µmol m^{-2} s^{-1} was considered for all PBRs [41]. To verify this light intensity and to find a range for flow rates, microalgae have been cultivated using 0.04% and 15% CO_2 and under the light intensities of 40, 80, 130 and 165 µmol m^{-2} s^{-1} and flow rates of 100, 200, 500, 1000 and 1500 mL min^{-1} (data not shown). Finally, light intensity of 165 µmol m^{-2} s^{-1} and flow rate range of 50–150 mL min^{-1} were selected for the main experiments as microalgae were not able to grow well under the flowrates of 500–1500 mL min^{-1} due to high acidity of culture.

To assess the effect of CO_2 concentration, flow rate and PBRs' diameters on microalgal growth, CO_2 mitigation, and nutrient removal, a full factorial design with three center point was employed by Minitab software (2018). Three numeric factors with three levels were examined which are shown in Table 1. All the experiments were accomplished in triplicates and data are shown as mean ± standard deviation in tables and error bars in graphs.

Optimization and Prediction by Artificial Neural Network and Support Vector Regression Methods

The effects of CO_2 concentration, flowrate, reactor diameter and cultivation time on the biomass concentration have been predicted by Artificial Neural Network (ANN) and Support Vector Regression (SVR) methods. The artificial neural network output is defined in Eq. (5) by processing the input information in a parallel process [45, 46].

$$Z_j = f\left(\sum_{i=1}^{Ni} [wu + b]_i\right) \tag{5}$$

where f is the operating function, Ni is the number of inputs, w is the connection weights, b is the bias, u and Z are the *ith* input and *jth* output of an ANN, respectively. The Multi-Layer Perceptron (MLP) could be a feed-forward artificial neural network that can perform a non-linear mapping with arbitrary accuracy [47]. The Levenberg–Marquardt algorithm is used as a learning algorithm for the training of experimental data to achieve a proper model by selecting the number of layers and neurons [48, 49].

Support Vector Machine (SVM) is used for arrangement and regression purposes and optimization of variable y_i which is a function of several independent variables x_i. The relationship between independent and dependent variables is obtained by an algebraic function such as y = f (x), which is as follows:

$$f(x) = w^T.\phi(x) + b \tag{6}$$

where w is the weights vector, b is the bias factor and ϕ is also a kernel function and the goal is to find a functional form of $f(x)$.

This can be achieved by training a SVR model by a set of data which the model operation basis has been previously discussed [48]. Briefly, the characteristics of w and b in the SVR model are calculated using the Karush–Kuhn–Tucker theory conditions same as Eq. (7):

$$W = \sum_{i=1}^{N} \phi(x_i)\left(\alpha_i^+ - \alpha_i^-\right) \tag{7}$$

where α is the Lagrange coefficient and $\phi(x)$ is the core function. Calculation of $\phi(x)$ is very complicated and thus to solve this, a Kernel function is defined in Eq. (8):

$$K(x_i.x_j) = \left(\phi(x_i).\phi(x_j)\right) \tag{8}$$

Different kernels (linear, quadratic, Gaussian, logistic, and polynomial) are used for a backup vector regression model and the model parameters along with the kernel parameter were calculated.

To design and create an appropriate model, the correlation coefficient, and Root Mean Square Error (RMSE) were utilized for the assessment of the results. The square of the correlation coefficient "R^2" and RMSE are characterized as:

$$R^2 = 1 - \frac{\sum_{i=1}^{N}\left(Y_{Exp} - Y_M\right)^2}{\sum_{i=1}^{N}\left(Y_{Exp} - \overline{Y_{Exp}}\right)^2} \tag{9}$$

$$RMSE = \sqrt{\frac{\sum_{i=1}^{N}\left(Y_{Exp} - Y_M\right)^2}{N}} \tag{10}$$

where, Y_{Exp} and Y_M are the values of experimental and model predictions, respectively and N is the amount of data.

Results and Discussions

Biomass Growth of C. vulgaris

The biomass growth of microalgae *C. vulgaris* for all 11 experiments (carried out in three PBRs) is plotted in Fig. 2. As can be seen, experiments that were supplied with CO_2 demonstrated a higher growth compared to ones supplied with air. The maximum cell concentrations achieved in all three PBRs were 3.15, 3.63 and 3.23 g L^{-1} for PBR 1 (15%

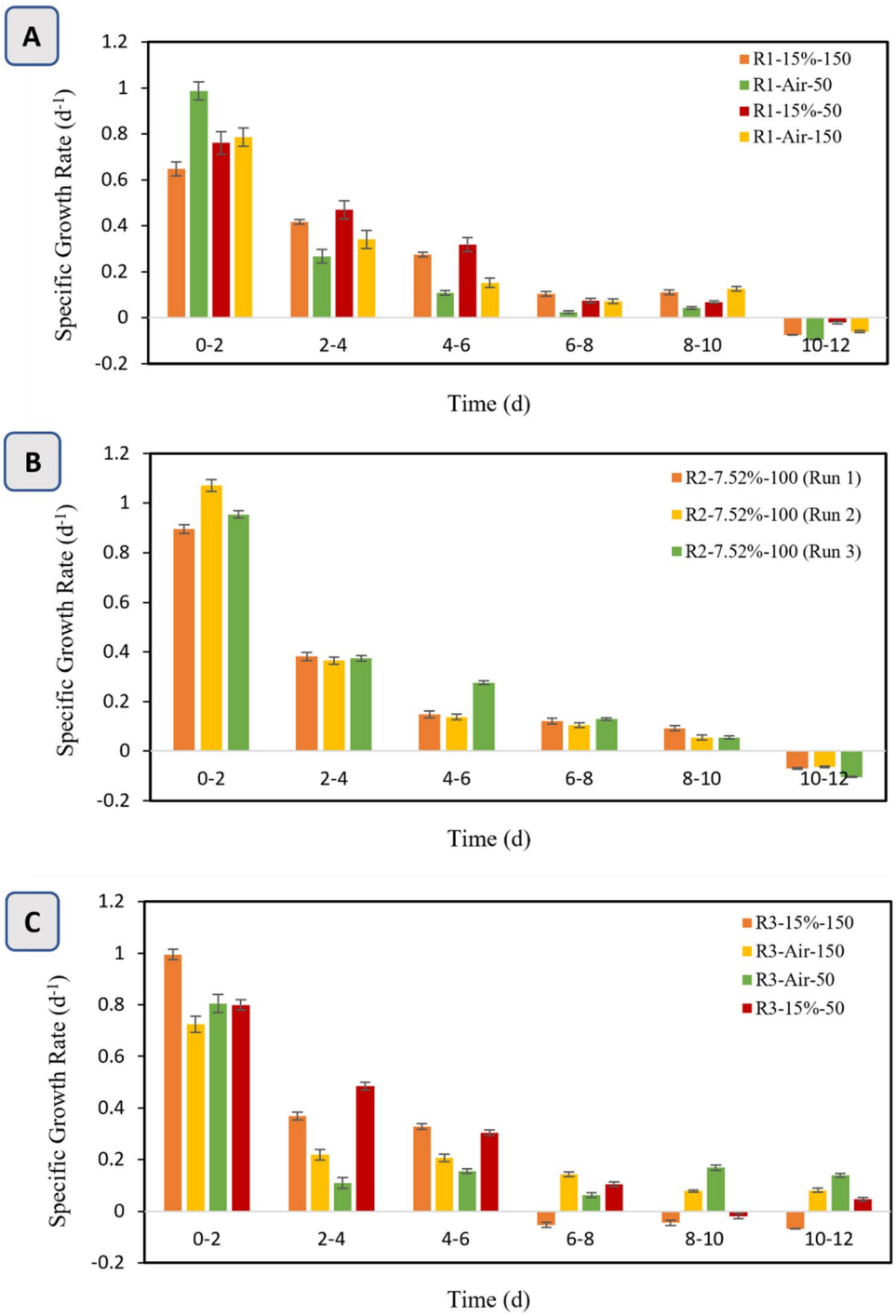

Fig. 3 Specific growth rate of *C. vulgaris* for **A** PBR1, **B** PBR2, **C** PBR3

CO_2 concentration, 50 mL min^{-1} flow rate), PBR 2 (7.52% CO_2 concentration, 100 mL min^{-1} flow rate) and PBR 3 (15% CO_2 concentration, 150 mL min^{-1} flow rate) respectively; while maximum biomass concentrations achieved for PBR 1 and 3 using 0.04% CO_2 were 1.92 and 2.2 g L^{-1}, respectively.

Although this experiment showed that *C. Vulgaris* can grow well in different CO_2 concentrations and flow rates, the biomass concentration, productivity and specific growth rate are greatly influenced by the cultivation conditions. This observation is in accordance with the work carried out by Anjos et al. [29].

As illustrated in Fig. 2A *C. vulgaris* had a similar growth for aerations of 50 and 150 mL min^{-1} and CO_2 concentrations of 0.04% and 15% until the day 5 in PBR1; However, from day 6, the run with 15% CO_2 concentration and 50 mL min^{-1} flow rate grew drastically and reached the maximum concentration of 3.15 g L^{-1} at day 9. Microalgal cells

Table 2 Summarization of maximum biomass concentration, maximum biomass productivity and maximum specific growth rate of *C. vulgaris* under different CO_2 concentrations, flowrate and different bioreactor diameter

Reactor No	Cultivation conditions			Growth parameters		
	Column diameter (cm)	CO_2 concentration (%)	Flow rate (mL/min)	$X_{max}(g.L^{-1})$	$P_{max}(gL^{-1}d^{-1})$	$\mu_{max}(day^{-1})$
Reactor 1	7	0.04	50	1.75 ± 0.16	0.31 ± 0.05	1.40 ± 0.03
		0.04	150	1.92 ± 0.16	0.24 ± 0.06	1.14 ± 0.05
		15	50	3.15 ± 0.13	0.35 ± 0.02	1.34 ± 0.04
		15	150	2.29 ± 0.20	0.23 ± 0.06	0.82 ± 0.04
Reactor 2	10.5	7.52 (1st Run)	100	3.45 ± 0.17	0.38 ± 0.06	1.04 ± 0.13
		7.52 (2nd Run)	100	3.20 ± 0.23	0.43 ± 0.07	1.60 ± 0.19
		7.52 (3rd Run)	100	3.63 ± 0.18	0.43 ± 0.05	1.03 ± 0.14
Reactor 3	14	0.04	50	1.79 ± 0.16	0.25 ± 0.07	1.26 ± 0.12
		0.04	150	2.20 ± 0.11	0.33 ± 0.03	1.31 ± 0.10
		15	50	3.13 ± 0.17	0.38 ± 0.06	0.83 ± 0.16
		15	150	3.25 ± 0.21	0.49 ± 0.08	1.42 ± 0.20

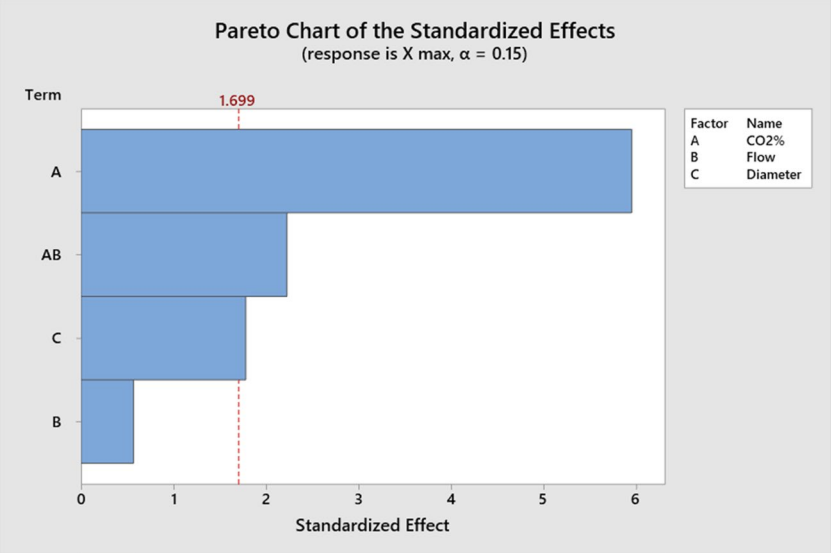

Fig. 4 Effectiveness of experimented parameters on microalgal growth

are approximately comprised of 50% carbon by dry weight and the carbon is regarded as a limiting nutrient in wastewaters or culture media [50]. In other words, sparging CO_2 bubbles to the culture, improves the carbon mass transfer to the liquid and increasing the CO_2 concentration and boosting gas flow rate also raise the mass transfer rate to a higher extent [28, 51]. Consequently, it is expected that microalgal growth will be enhanced by the addition of carbon dioxide to the culture medium. On the other hand, a high CO_2 content in the liquid can reduce the culture pH and leads to negative changes in cells physiology and growth [28]. Based on the aforementioned reasons, in the experiment with 15% CO_2 concentrations and the flow of 150 mL min^{-1}, high amounts of CO_2 reduced the culture pH and therefore less growth was observed than the experiment with the 15% CO_2 and 50 mL min^{-1} flow. These results are in a good agreement with the results of study by Liu et al. [28], which they cultured *C. vulgaris* in wastewater and used CO_2 concentration range from 1 to 20%. They concluded that at 10% CO_2 concentration, *C. vulgaris* reached to the maximum biomass concentration of 1.12 g L^{-1}, while growth dropped at 20% CO_2 concentrations due to low pH of culture.

CO_2 concentrations of 0.04% (air) and 15% and flow rates of 50 and 150 mL min^{-1} resulted in a non-similar growth rate of microalgae. Same as PBR 1, experiments with the injection of 15% CO_2 concentration to PBR3 resulted in a higher cell growth, while on the contrary to PBR 1, higher growth for 150 mL min^{-1} of flow rate was observed. The reason can be attributed to the larger volume of PBR 3 than PBR 1 (16–4 L) in which cells demanded more carbon content that could be satisfied with higher flow rates. Besides, in reactor 3 with a larger diameter, cells were receiving less

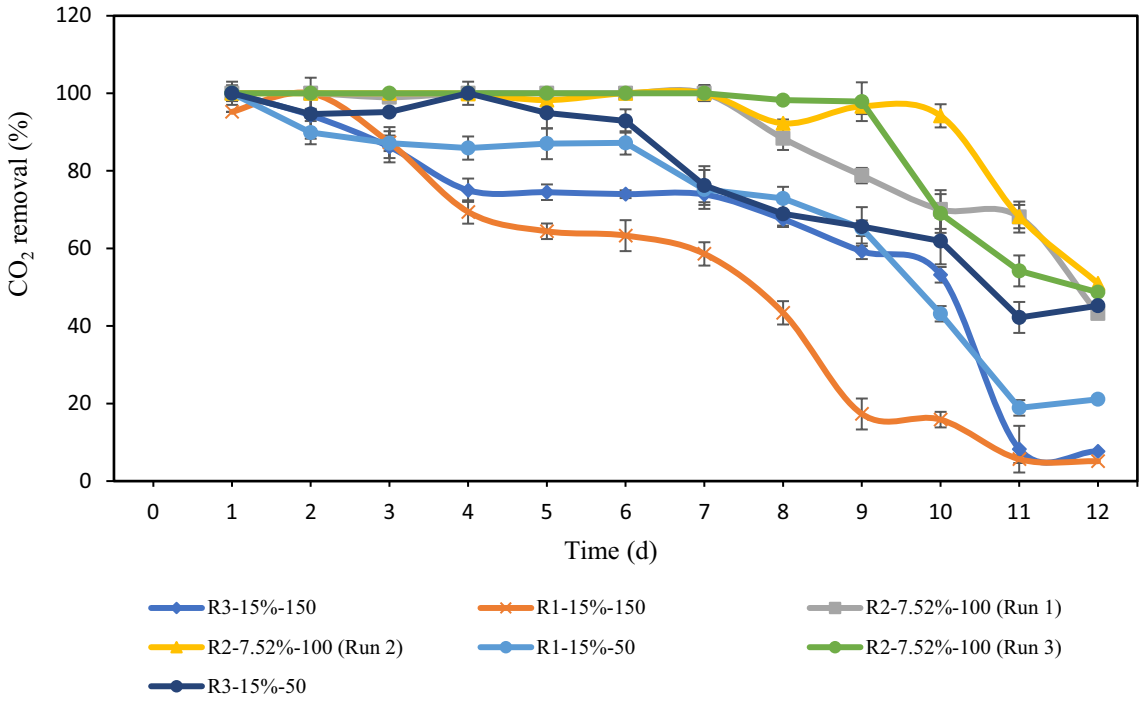

Fig. 5 Daily CO_2 removal efficiency of *C. vulgaris* vs. time

light than reactor 1 and therefore, a higher flowrate boosted liquid circulation through the column and consequently, cells received more light energy from being moved adjacent to the bioreactor's wall [29]. This phenomenon is also observable for experiments with injection of air (0.04% CO_2) where biomass concentration reached to the final value of 2.20 and 1.79 g. L^{-1} at the flowrates of 150 and 50 mL min^{-1}, respectively. Such results are in accordance with the results of Ryu et al. [52] in which *Chlorella sp.* AG10002 concentration raised by ~ 35% by increasing the flow rate from 0.06 vvm to 0.4 vvm. As can be seen in Fig. 3, cell growth experiment with 15% CO_2 and 150 mL min^{-1} dropped at day 6, which can be attributed to the fact that cells were receiving less light, since at such a high cell concentration, dark zones dominated the column and self-shading phenomenon happened. Self-shading occurs in dense algal cultures, which decrease the amount of light available for individual cell and prevents algal growth and CO_2 biofixation [53–55].

All the experiments were accomplished at the center point (7.5% CO_2 concentration and 100 mL min^{-1} flow rate) for the reactor 2. *C. vulgaris* showed a higher growth than the experiments in reactor 1 and reactor 3, with the highest biomass concentration of 3.63 g L^{-1}. These results imply that cells received sufficient light energy as the reactor's diameter was not as large as reactor 3 to create self-shading and also the carbon content has not exceeded to the extent that reduce the culture's pH to the point that inhibits the growth.

The specific growth rate for each experiment was estimated based on Eq. (3) and are shown as 2-days intervals in Fig. 3A–C. Generally, the highest specific growth rate in this study was observed at the first intervals due to high nutrient content in the culture media and the fact that cells were receiving the highest light energy during the cultivation period as the media was transparent initially. On the other hand, by depleting culture from nutrients and due to the culture becoming translucent, specific growth rate decreased gradually with time. However, in some cultures, especially for the ones which dosed with a high CO_2 content, it took one day for algal cells to be adapted to the conditions. Comparing the specific growth rates in all experiments, shows that higher amount of nutrients available in reactors 2 and 3 in comparison to reactor 1, made the conditions more favorable for algal growth in the first two days.

Table 2. Shows the Final biomass concentrations (X_{max}), maximum biomass productivity (P_{max}) and maximum specific growth rate (μ_{max}) of *Chlorella vulgaris* under different CO_2 concentration, flow rates in different bioreactors. Highest values are observable for reactor 2 as favorable conditions had been provided for cells to grow. Also, generally experiments with higher CO_2 concentrations and higher flow rates resulted in a higher productivity and biomass concentration. One factor affecting higher growth, is repressing the oxygenating activity of Rubisco and higher activity of carboxylating enzyme due to CO_2 addition [56]. Minitab results (Fig. 4) also showed that CO_2 concentration, its interaction

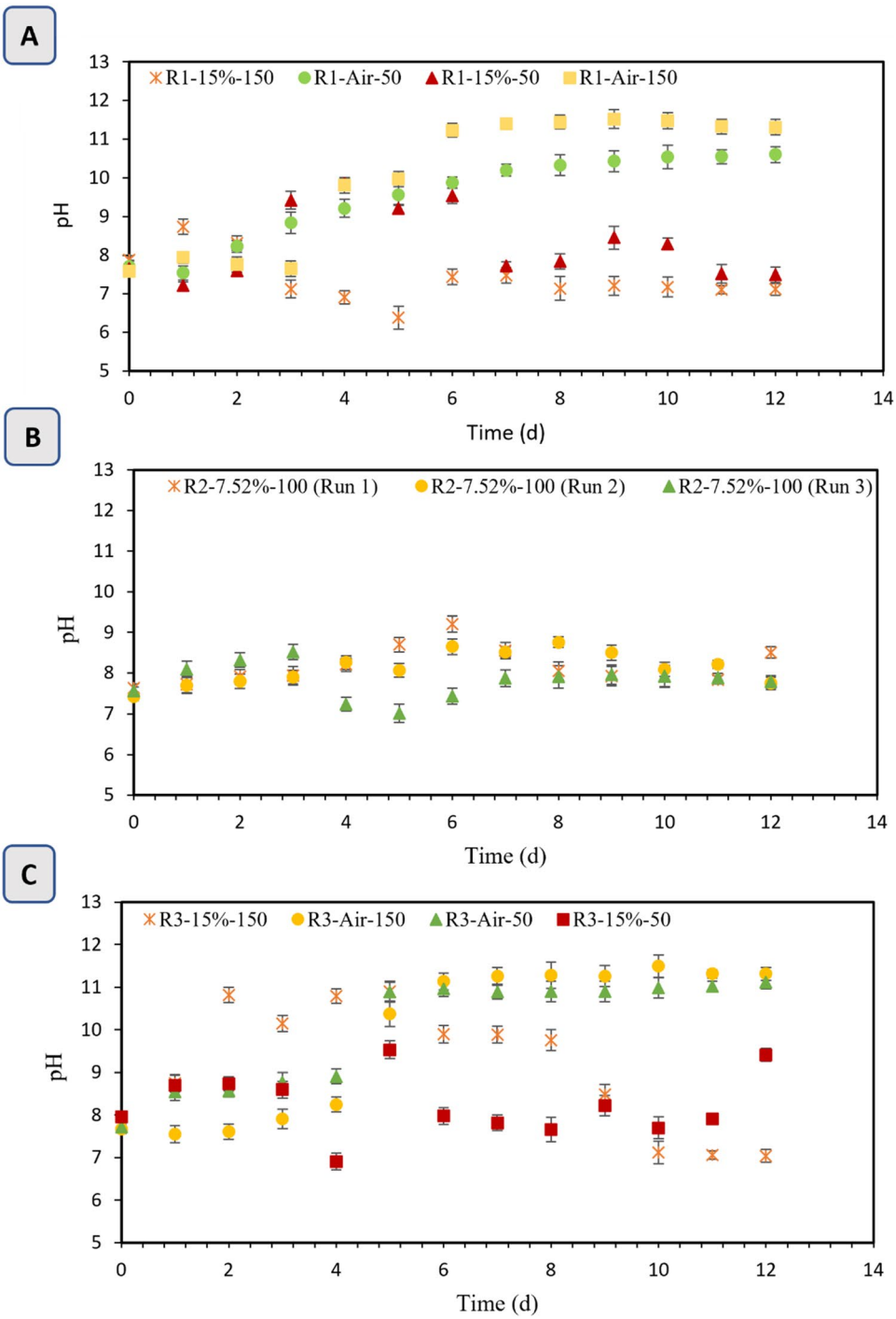

Fig. 6 pH values during the cultivation period in **A** PBR 1, **B** PBR2, **C** PBR3

with flowrate and bioreactor's diameter were influencing parameters on the algal growth, respectively.

CO_2 Removal Efficiency

CO_2 gas is injected in the reactors as the carbon source and Fig. 5 shows the CO_2 removal efficiencies in PBRs 1, 2 and 3. By sparging CO_2 gas into the reactors, gas bubbles start to raise in the column and carbon in the bubble diffuses through the gas–liquid interface and dissolves in the liquid. It is important to mention that by the dissolution of CO_2 in the liquid, the dissolved inorganic carbon (DIC) content increase in the forms of CO_2, H_2CO_3, HCO_3^- and CO_3^{2-}, which are usually in equilibrium [57] and consumed by microalgae. In fact, photosynthesis is happening in chloroplast where inorganic carbon (Ci) transporters and cell membrane transporters are located [5]. It is assumed that the amount of organic carbon in the experiment is negligible

Table 3 Daily and average CO_2 removal efficiency of PBRs 1, 2 and 3

Time (d)	1	2	3	4	5	6	7	8	9	10	11	12	Avg. CO_2 removal (%)
R1-15%-50	100.0 ± 0	89.9 ± 2	87.1 ± 3	85.9 ± 2	87.0 ± 3	87.2 ± 4	75.2 ± 3	72.9 ± 5	65.2 ± 3	43.2 ± 2	18.9 ± 2	21.1 ± 2	69.5
R1-15%-150	95.2 ± 3	100.0 ± 0	87.3 ± 4	69.4 ± 4	64.4 ± 3	63.3 ± 2	58.6 ± 4	43.4 ± 3	17.3 ± 3	15.9 ± 4	5.7 ± 2	5.1 ± 1	52.1
R2-7.52%-100 (Run 1)	100.0 ± 0	100.0 ± 0	99.0 ± 0	100.0 ± 0	100.0 ± 0	100.0 ± 0	100.0 ± 0	88.4 ± 2	78.8 ± 1	70.1 ± 2	68.1 ± 3	43.2 ± 3	87.3
R2-7.52%-100 (Run 2)	100.0 ± 0	100.0 ± 0	100.0 ± 0	99.9 ± 0	98.3 ± 0	100.0 ± 0	100.0 ± 0	92.3 ± 2	96.7 ± 1	94.2 ± 2	68.2 ± 2	51.0 ± 3	91.7
R2-7.52%-100 (Run 3)	100.0 ± 0	100.0 ± 0	100.0 ± 0	100.0 ± 0	100.0 ± 0	100.0 ± 0	100.0 ± 0	98.2 ± 0	97.9 ± 0	69.0 ± 5	54.2 ± 5	48.7 ± 4	89.0
R3-15%-50	100.0 ± 0	94.6 ± 2	95.2 ± 1	100.0 ± 0	94.9 ± 3	92.9 ± 4	76.2 ± 3	68.9 ± 5	65.6 ± 3	61.9 ± 5	42.2 ± 6	45.2 ± 4	78.1
R3-15%-150	100.0 ± 0	94.3 ± 3	86.2 ± 6	75.0 ± 4	74.5 ± 3	74.0 ± 2	73.9 ± 1	67.5 ± 2	59.3 ± 2	53.2 ± 2	8.3 ± 2	7.7 ± 3	64.5

and *C. Vulgaris* mainly uses DIC as the carbon source [28]. However, the availability of different forms of inorganic carbon in the culture media is a function of culture pH. In fact, in a low pH, DIC is usually in the forms of CO_2 and HCO_3^{2-} and in normal or slightly alkaline pH is majorly in the form of HCO_3^- and microalgae prefer to uptake CO_2 in passive diffusion rather than active transport in the form of HCO_3^- [58–60]. Consequently, the carbon dioxide bio-fixation and microalgae growth are directly influenced by culture pH [28]. Figure 6A–C show the pH of culture in reactors 1–3 in the 12-days cultivation of *C. vulgaris*.

Through the process of CO_2 dissolution in the medium, some of the carbon dioxide is dissolved in the medium and utilized by microalgae. Reduction of culture pH has occurred due to the dissolution of CO_2 in the culture medium and is increased by the uptake of microalgae. However, at the conditions where the rate of CO_2 injection is higher than the rate of CO_2 consumption by microalgae (i.e. high CO_2 concentrations and high flow rates), carbon remains in abundance and results in the precipitation of dissolved salts and therefore scarcity of nutrients for microalgae [61]. As the CO_2 injection continues, less carbon dioxide is diffused into the liquid and by the less growth of microalgae due to the unfavorable pH of the culture and insufficiency of nutrients, the majority of the CO_2 is wasted by escaping from the photobioreactor.

Hence, CO_2 removal and biofixation in the reactor is not only microalgal species specific and its ability to assimilate carbon, but also depends on the photobioreactor design, geometry, and other operational factors such as CO_2 concentration, gas flow rate, sparger design, light intensity etc.

As can be seen in Fig. 5, CO_2 removal efficiency for all the experiments were almost 100% at the first day of cultivation. By the dissolution of CO_2 in the culture medium and increasing the carbon composition in the liquid phase, the mass transfer gradient between the bubble and liquid reduces and thus, results in the less carbon removal efficiency. Also, we observed that the removal efficiency of the experiments is associated with the specific growth rates of microalgae. The higher specific growth rate of microalgae means a greater number of cells available in the media and therefore higher carbon uptake which in turn results in greater carbon gradient between the bubbles and the culture media and contribute to higher mass transfer and carbon removal efficiency. In this case, experiments with the injection of 7.5% CO_2 and flow of 100 mL min^{-1} had a better efficiency for CO_2 removal and the efficiency of 100% observed until the seventh day of cultivation. Experiments with the CO_2 concentration of 15%, on the other hand, had lower efficiency due to lower growth rate of microalgae and the fact that the medium reaches to the saturation point sooner [62]. Besides, by comparing the experiments with 15% CO_2 injection and flowrates of 50 and 150 mL min^{-1} we observed that CO_2 removal efficiency in the experiments with 50 mL min^{-1} had

Table 4 Previous research on biomass growth and CO_2 removal optimization

Microalgae strain	Cultivation system	Reactor volume (L)	CO_2 concentration range (%)	Optimal CO_2 concentration (%)	Highest biomass concentration (g. L^{-1})	CO_2 fixation rate (g. L^{-1}. d^{-1})	CO_2 removal efficiency %	References
Chlorella sp.	Cylindrical reactor	0.8		2	1.211		58	[64]
Chlorella sp.	Mini raceway pond	8	1,5 & 10	10	2.25	–	46	[65]
C. vulgaris LEB-104	BioFlo fermentor	8	5	–	1.94	0.25164 (g/l.d)	–	[66]
Chlorella sp. NCTU-2	Porous centric-tube column	–	5	–	3.46	–	35	[67]
Chlorella sp. NCTU-2	Bubble column	4	5	–	2.37	–	24	[67]
C. vulgaris	Membrane-sparged helical tubular photobioreactor	0.8	0.093	–	0.95	3.55 g L^{-1} d^{-1}		[68]
C. vulgaris	Flask	0.2	1 to 20	10	1.12	–	–	[28]
C. vulgaris P12	Flask	0.09	2 to 10	6.5	10	2.22 g L_1 d_1	–	[29]
Chlorella pyrenoidosa	Bubble column photobioreactor	0.4	3 to 10	5	1.6	–	–	[69]
C. vulgaris	Bubble column photo-bioreactor	1	3 to 11	7	4.2	0.633	–	[61]

higher efficiency. This observation can be attributed to the fact that higher flowrates mean larger superficial gas velocity and as the superficial gas velocity increase in the bioreactor, the bubbles residence time reduces and therefore, CO_2 fixation decreases.

Table 3 shows the daily and average CO_2 removal efficiencies of PBRs 1, 2 and 3. As can be seen in Table 3, maximum CO_2 removal efficiency observed at the CO_2 concentration of 7.5% and flow rate of 100 mL min^{-1} with the average of 91.7%. Obtained results are in good agreement with the results of previous studies. The maximum CO_2 fixation rate was observed at 10% CO_2 for both *Chlorella pyrenoidosa* and *Spirulina obliquus* using CO_2 concentrations of 0.03%, 5%, 10%, 20%, 30%, 50% [57]. In a similar work, Anjos et al. [29], studied the CO_2 fixation rate of *Chlorella vulgaris* in CO_2 concentrations of 2%, 6% and 10% and the aeration rates of 0.1, 0.4 and 0.7 vvm and observed the maximum CO_2 fixation rate of 2.22 g. $L^{-1}.d^{-1}$ at 6% CO_2 concentration. Li et al. [63], indicated that increasing gas flow rate from 0.05 to 0.5 vvm, reduced the carbon removal efficiency and they obtained maximum CO_2 removal efficiency of *S. obliquus WUST4* with 67% by the provision of 12% CO_2 concentration.

Table 4 summarizes the previous research, accomplished on the growth and CO_2 removal efficiency/biofixation of *Chlorella* strain in various CO_2 concentration, flow rates and photobioreactor types. As CO_2 removal is a function of various operational and photobioreactor parameters, optimization of all factors should be considered to achieve maximum microalgal growth and CO_2 removal efficiency. It is noteworthy to mention that, generally, smaller size reactors have higher biomass concentration as can also be seen in the table while, reaching to a high cell concentration in large reactors is challenging. Based on the results obtained in our experiments, and considering the larger volumes of reactors, achieving a higher cell concentration of and CO_2 removal efficiency simultaneously, compared to the literature, implies that bioreactors were operating in optimal conditions.

Nitrogen and Phosphorus Removal

Nitrogen is one of the most essential nutrients for microalgal growth which is involved in the major metabolic pathways of microalgae and is used for chlorophyll synthesis as well as protein production inside the cell. Low amounts of nitrogen in the culture hinders cellular activities and therefore lower the cell growth [70].

The total nitrogen (TN) in the culture posed a significant reduction trend for all experiments which are shown in Fig. 7A–C. The initial nitrate level was around 1070 ppm for all the experiments. Hariz et al. [62] has found no correlation between CO_2 fixation and TN reduction; However, other researches [71, 72], claimed that the concentrations of nitrogen and phosphorus have abated due to microalgal

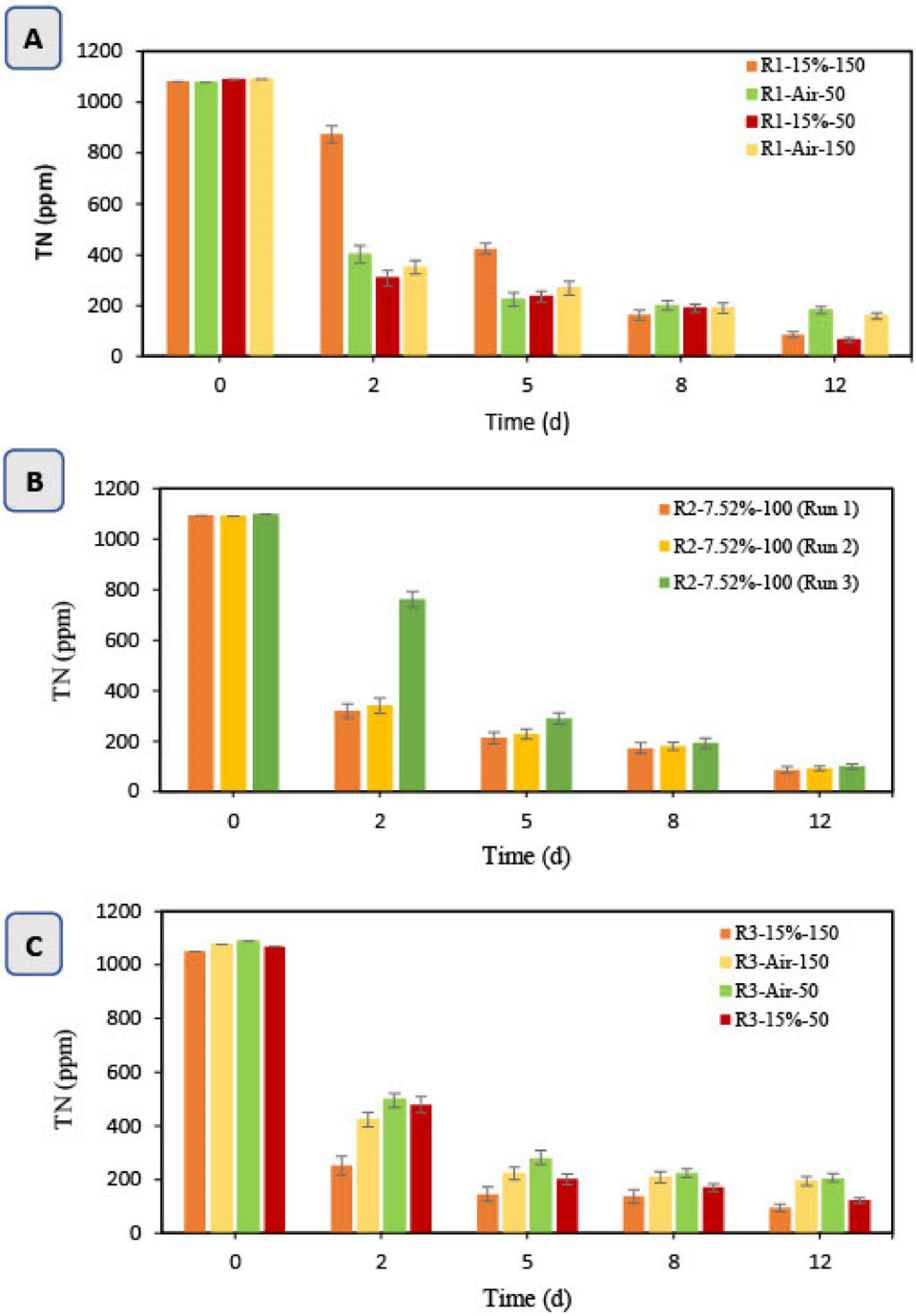

Fig. 7 Total nitrogen concentration (ppm) in 12-days cultivation of *C. vulgaris* in **A** PBR 1, **B** PBR2, **C** PBR3

growth. While low aeration and inappropriate agitation may induce poor distribution of nutrients through the culture media and therefore ineffective nutrient removal [62], in this study, high nitrogen and phosphorus removal efficiency achieved. According to Table 5, nitrogen removal efficiency of all experiments was in the range of 81–94% in which the maximum value achieved for reactor 1 operating at 50 mL min^{-1} and 15% CO_2 concentration. It is noteworthy to mention that nitrogen volatilization might happen at pH above 8 [73] that might have happened due to the fast growth of microalgae or low rate CO_2 injection. Madigan et al. [74], observed that *C. vulgaris* uptakes nitrogen and utilizes in its cell components, while the rest is oxidized into N_2 and discharged into the atmosphere.

The total phosphorous (TP) concentration decreased with time, in all the experiments. Figure 8A–C show the trend of TP removal in 12-days cultivation period. The initial concentration of TP was 21 ppm approximately and almost depleted within 5 days for all experiments. Such results are in accordance to previous researches. Hariz et al. [62],

Table 5 Maximum nitrogen removal efficiency in 12 days of cultivation

Reactor No	Column diameter (cm)	CO_2 concentration (%)	Flow rate (mL/min)	Maximum nitrogen removal efficiency (%)
Reactor 1	7	0.04	50	83.1
		0.04	150	85.4
		15	50	94.1
		15	150	92.0
Reactor 2	10.5	7.52 (1st Run)	100	92.1
		7.52 (2nd Run)	100	91.5
		7.52 (3rd Run)	100	90.9
Reactor 3	14	0.04	50	81.5
		0.04	150	81.9
		15	50	88.5
		15	150	91.0

assessed the effect of inoculum concentration (10–30% v/v), CO_2 concentration (10–25% v/v) and inlet gas flow rate (500–2000 mL min^{-1}) on the growth of *Chlorella* sp. cultured in the palm oil mill effluent with the initial TN of 330 ± 30 and observed 28–92% reduction in total nitrogen, while 80.9% TN reduction predicted at the optimum operational condition. Rasoul-Amini et al., also investigated the biomass productivity and TN reduction of five microalgal species and found 84.11% and 100% N and P uptake, respectively, for *Chlorella* sp. with the initial nitrate concentration of 190.7 ± 0.12 mg. L^{-1} d^{-1}. Similarly, same results were observed for Caporgno et al. [75] which achieved 99% and 98% P removal efficiency for *Chlorella kessleri* and *Chlorella vulgaris* respectively, cultured in urban wastewater. Although similar trend and removal observed for phosphorus in this work and previous studies, higher TN removal efficiency in this work demonstrates a desired bioreactor design and efficient mixing while the initial TN concentration was much higher than other studies.

Light Intensity Distribution Inside Photobioreactors

Light intensity is one of the most important determinants of microalgal photosynthesis. Microalgal growth is a function of light availability which is the primary limiting component in photobioreactor performance [76]. However, light availability is attenuated as the light passes through the bioreactor and therefore measured light intensity on the outer surface of the photobioreactor will not determine the incident light energy provided for the cells.

The observed light intensities in the cell suspension of *C. vulgaris* at the sixth day of cultivation in various light path lengths, are plotted in Fig. 9A–C for PBRs 1, 2, and 3, respectively. Light path length is the space between the light source and the desired spot. According to Fig. 9A–C, as the light passes through the culture medium, it is attenuating due to availability of cells and interaction with the medium and bubbles [77]. As can be seen in Fig. 9A, light intensity was abated from 170 to 25.1 μmol m^{-2}. s^{-1} for the experiment with the highest biomass concentration (15% CO_2 concentration and 50 mL min^{-1} flowrate). The higher the biomass concentration in the culture medium, the higher light attenuation. Similar pattern is observed for the reactors 2 and 3 in which light availability was reduced from 172 to 8.9 μmol m^{-2} s^{-1} and 174 to 0 μmol m^{-2} s^{-1} for the highest biomass concentration experiments for reactor 2 (7.5% CO_2 concentration and 100 mL min^{-1} flowrate) and 3 (15% CO_2 concentration and 150 mL min^{-1} flowrate), respectively. A high surface area as well as cell productivity are two characteristics that should be considered to determine the performance of a microalgal cultivation system to be cost-effective. Thus, results obtained suggest that cells at the center of the reactor 3 were not receiving adequate light energy and therefore, the designed photobioreactor 3 is not suitable for algal cultivation, though a relatively high cell concentration achieved due to the proper mixing efficiency in this photobioreactor.

Moreover, bubbles in the culture act as optical lens and scatter the light inside the bioreactor and therefore, increase in flowrate reduce the light availability in the column [78]. Khichi et al. [79], observed an increase in self-shading at the

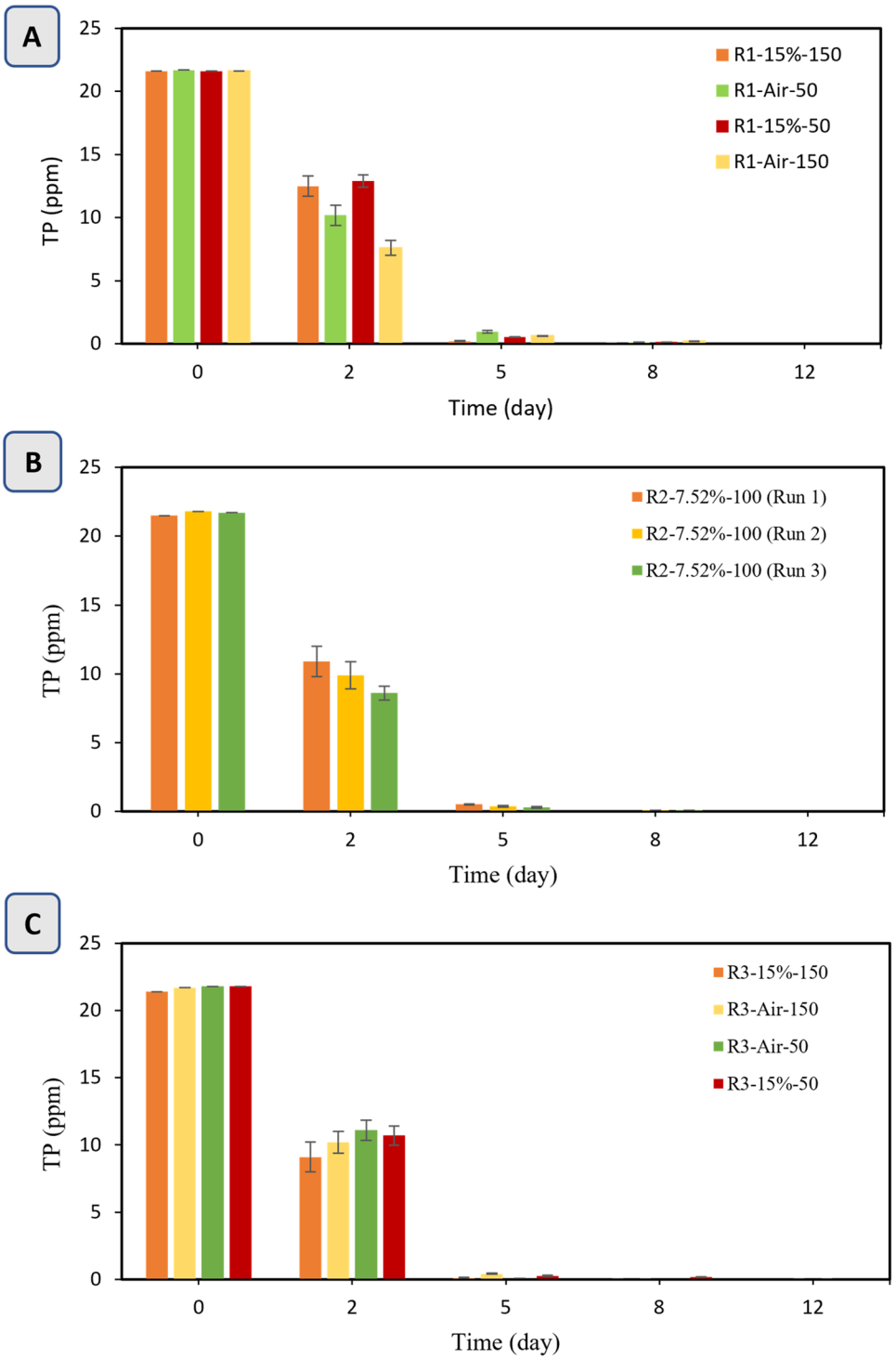

Fig. 8 Total phosphorus concentration (ppm) in 12-days cultivation of *C. vulgaris* in **A** PBR 1, **B** PBR2, **C** PBR3

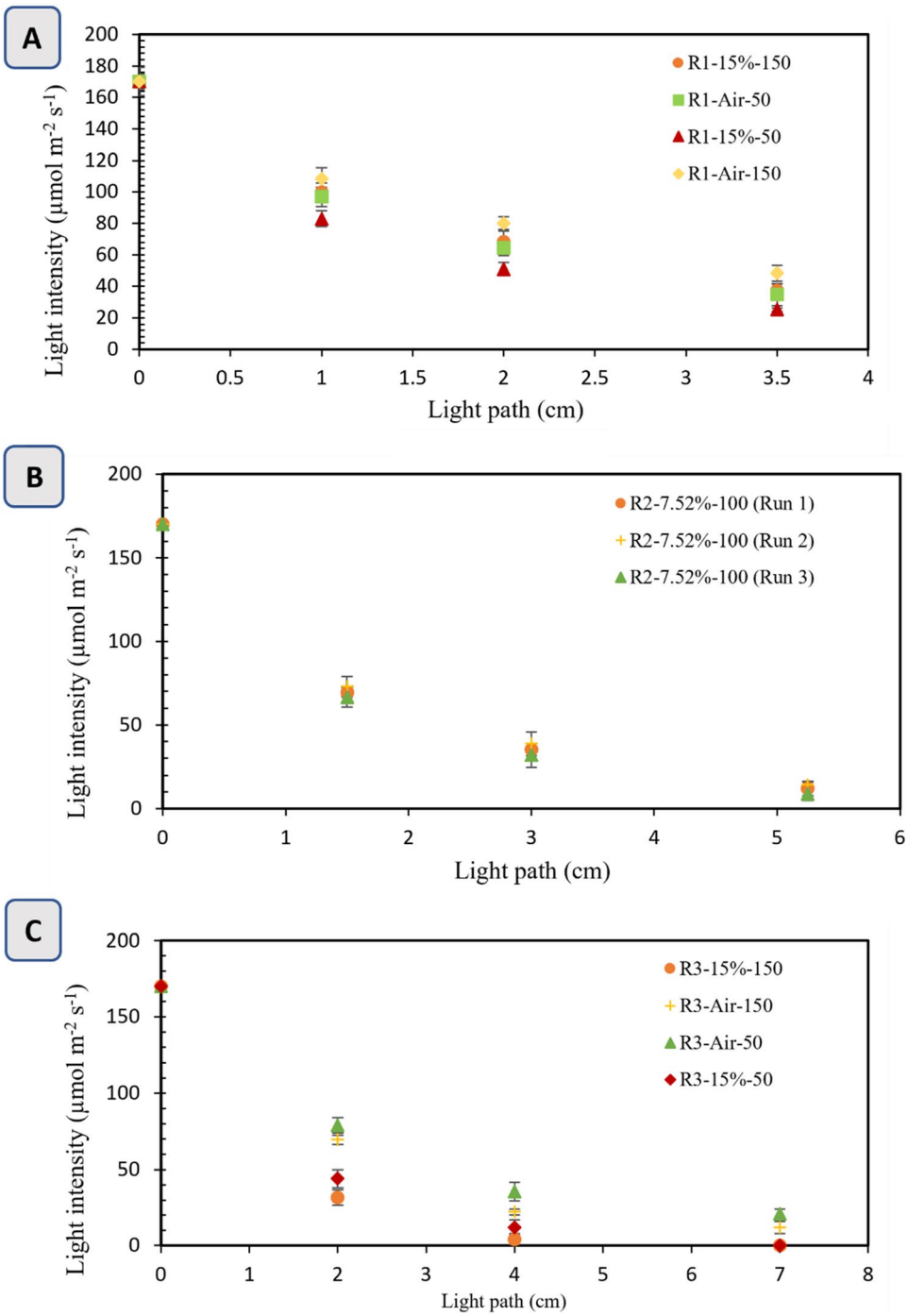

Fig. 9 Light intensity vs. light path inside **A** PBR 1, **B** PBR2, **C** PBR3

higher cell concentrations which results in less light penetration inside the reactor. Obtained results are in good agreement with the observations of other studies. Naderi et al. [80], studied the modelling of light intensity distribution inside a rectangular and cylindrical algal photobioreactors and various light intensities and observed 92% decrease at the cell concentration of 1.34 g L^{-1} in light attenuation in the first 2 cm of the reactor. Kumar et al. [81] claimed that local light intensity information is advantageous to assess the photobioreactor's design efficiency and attained the same exponential attenuation for light availability in the reactor.

Modeling and Prediction Using SVR and Neural Network

To determine the effect of CO_2 Concentration, gas flow-rate, reactor diameter and time on the prediction of biomass concentration behavior, 143 data set with various learning

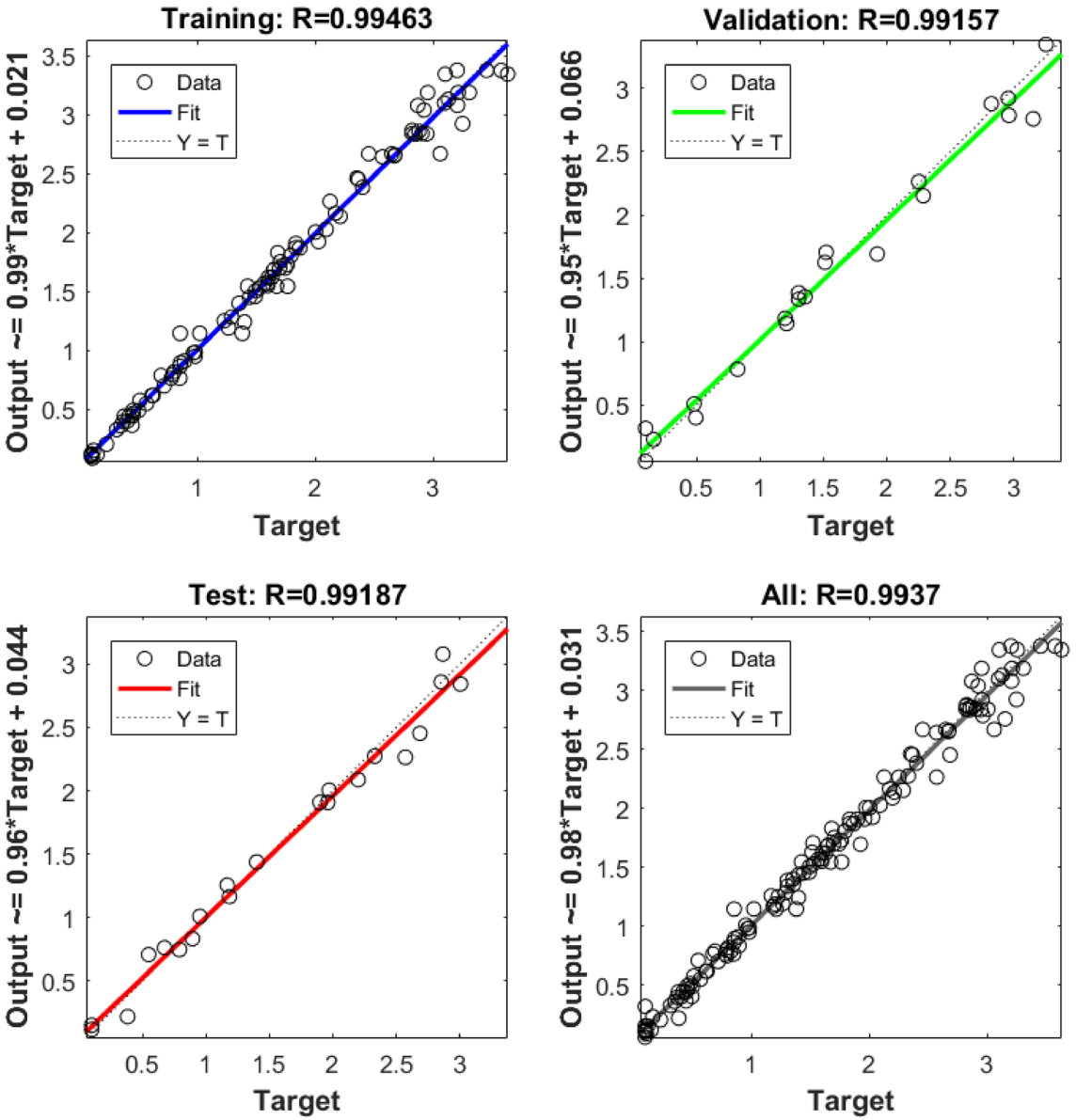

Fig. 10 MLP model predictions and experimental data

algorithms such as combined conjugate gradient algorithm (Traincgb), Bayesian algorithm (Trainrp), Levenberg–Marquardt algorithm (Trainlm), etc. were used for training MLP models. Results show that Levenberg–Marquardt with three hidden layers and 8, 15 and 8 neurons in the hidden layers is the best algorithm and structure for simulations. The experimental data was divided into three distinct sets including training (70%), validation (15%), and test data (15%) and the results of %AARE, RMSE, and R^2 were 1.3042, 0.0053, and 0.9937, respectively. Adaptation between the experimental data and the MLP model predictions for data training, validation and test is given in Fig. 10 and error bars for this network are shown in Fig. 11.

For the model prediction by SVR, WEKA 3.7 software was used. In this method, similar to the MLP method, 143 existing laboratory datasets have been used for modeling with random training test. The parameters γ, C, and ε were obtained by trial and error for different kernels (linear, quadratic, Gaussian, logistic). The best result is RBF kernel and the optimization parameters for this model have been shown in Table 6.

The results of SVR and MLP modeling showed that the use of two models has accurate estimations of experimental results; however, SVR method showed a higher accuracy.

The effects of different parameters such as CO_2 concentration, gas flowrate, reactor diameter and time on the

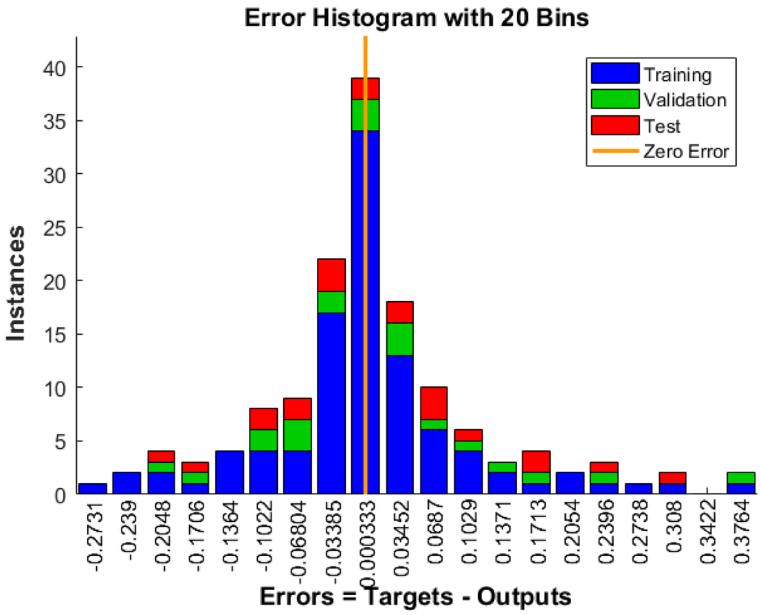

Fig. 11 Error bar for model predictions with experimental data

Table 6 Optimization of different parameters in WEKA software

Criteria Evaluation		Model parameters			Kernel type	Number of kernel evaluations	Number of training data
RMSE	R^2	ε	$\gamma = \frac{1}{2\sigma^2}$	C			
0.0307	0.9964	0.01	10	1	Gaussian (RBF)	10,296	143

prediction of biomass concentration have been investigated and shown in Fig. 12.

Figure 12A shows the effect of cultivation time and reactor's diameter on biomass concentration at a fixed CO_2 concentration and gas flowrate. Results show that increase in diameter increases the biomass concentration until a certain value, and hereafter, the higher the diameter, decreases the biomass concentration due to the self-shading. Investigation of the effect of reactor diameter and CO_2 concentration on the biomass concentration at a fixed flowrate and time is also shown in Fig. 12B. As the time was fixed at day 12 of the experiment, a high CO_2 concentration yielded a lower biomass concentration value, as the PBR is low in nutrients and therefore, the assessment is valid only for evaluating the reactors diameter on biomass growth. A sudden decrease in biomass concentration with an increase in reactor diameter is observable in Fig. 12C that shows the interaction of reactor's diameter and gas flowrate on biomass concentration, which is again due to the shadow effect. The interaction of CO_2 concentration and flowrate as well as the interaction of time and CO_2 concentration are shown in Fig. 12D and E, respectively. All the observations from Fig. 12 corroborate the results from previous studies.

Conclusion

In this study, performance of three bubble column photobioreactors was investigated through evaluation of maximum biomass concentration, CO_2 and nutrient removal after performing preliminary experiments to select the area of design. Microalgae *Chlorella vulgaris* as one of the best strains for the aim of biomass productivity with a high tolerance towards carbon dioxide were selected for this study. CO_2 concentration of power plant flue gas (ranging from 5 to 15%), light intensity at the saturation point of *Chlorella vulgaris*, flow rates range 50–150 mL min^{-1} and diameter of the photobioreactor in the range of 7–14 cm were considered as influential parameters on biomass productivity and CO_2 removal efficiency. The effects of CO_2 concentration, flowrate, reactor diameter and cultivation time on the biomass concentration were predicted by Artificial Neural Network (ANN) and Support Vector Regression (SVR) methods. Maximum cell concentration and CO_2 removal of 3.63 g. L^{-1} and 91.7% occurred for the reactor 2, with CO_2 concentration of 7.5%, flow rate of 100 mL min^{-1} and diameter of 10.5 cm. The Levenberg–Marquardt algorithm (three hidden layer with 8, 15 and 8 neurons) with correlation coefficient value of 0.9937 was selected as the optimal network. Also, the SVR by Gaussian kernel with correlation coefficient

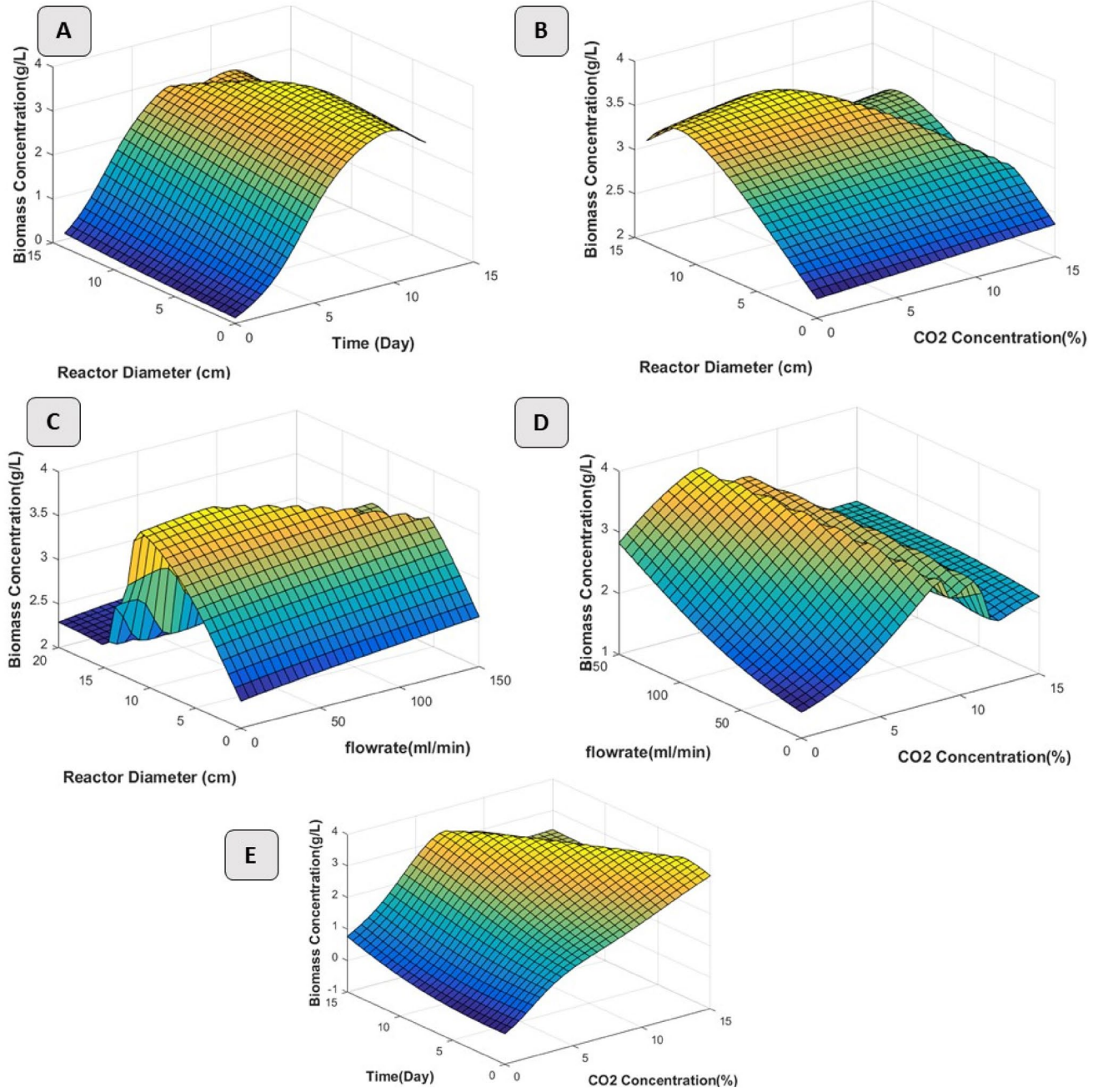

Fig. 12 SVR model prediction, **A** effect of cultivation time and reactor's diameter on biomass concentration at a fixed CO_2 concentration and gas flowrate **B** effect of reactor's diameter and CO_2 concentration on biomass concentration at a fixed time and gas flowrate **C** effect of reactor's diameter and gas flowrate on biomass concentration at a fixed CO_2 concentration and time **D** effect of cultivation CO_2 concentration and gas flowrate on biomass concentration at a fixed time and reactor's diameter **E** effect of CO_2 concentration and cultivation time on biomass concentration at a fixed reactor's diameter and gas flowrate

value of 0.9964 was fitted on the experimental data and results showed that two models have accurate estimations. Because of lower final biomass concentration in reactor with the diameter of 7 cm with respect to other reactors and self-shading phenomenon in reactor 3 it can be concluded that these two designs were not desired.

Acknowledgements The authors would like to thank the technical and financial support of Green Technology Laboratory at University of Tehran and Iranian National Algae Collection Center (INACC). Also thanks to Ms Baharan Ahmadi from University of Tehran for her assistance in analyzing and work in the lab.

Funding The authors have not disclosed any funding.

Data Availability The collected data can be handed out upon request.

Declarations

Conflict of Interest The authors have not disclosed any competing interests.

References

1. "Earth's CO2," 2022, [Online]. www.co2.earth.
2. Campbell, P.E., McMullan, J.T., Williams, B.C.: Concept for a competitive coal fired integrated gasification combined cycle power plant. Fuel **79**(9), 1031–1040 (2000)
3. Nduku Nzove, S.: Development and evaluation of performance of a bench scale Gasi er for sub-bituminous coal. JKUAT-COETEC (2021).
4. G. H. G. iEA: Building the cost curves for CO2 storage. Part (2002).
5. Nithiya, E.M., Tamilmani, J., Vasumathi, K.K., Premalatha, M.: Improved CO2 fixation with Oscillatoria sp. in response to various supply frequencies of CO2 supply. J. CO2 Util. **18**, 198–205 (2017)
6. Fernández, F.G.A., González-López, C.V., Sevilla, J.M.F., Grima, E.M.: Conversion of CO2 into biomass by microalgae: how realistic a contribution may it be to significant CO2 removal? Appl. Microbiol. Biotechnol. **96**(3), 577–586 (2012)
7. Diao, Y.-F., Zheng, X.-Y., He, B.-S., Chen, C.-H., Xu, X.-C.: Experimental study on capturing CO2 greenhouse gas by ammonia scrubbing. Energy Convers. Manag. **45**(13–14), 2283–2296 (2004)
8. Su, F., Lu, C., Cnen, W., Bai, H., Hwang, J.F.: Capture of CO2 from flue gas via multiwalled carbon nanotubes. Sci. Total Environ. **407**(8), 3017–3023 (2009)
9. Grimston, M.C., Karakoussis, V., Fouquet, R., Van der Vorst, R., Pearson, P., Leach, M.: The European and global potential of carbon dioxide sequestration in tackling climate change. Clim. Policy **1**(2), 155–171 (2001)
10. Pulz, O., Gross, W.: Valuable products from biotechnology of microalgae. Appl. Microbiol. Biotechnol. **65**(6), 635–648 (2004)
11. Skjånes, K., Lindblad, P., Muller, J.: BioCO2–a multidisciplinary, biological approach using solar energy to capture CO2 while producing H2 and high value products. Biomol. Eng. **24**(4), 405–413 (2007)
12. Hajinajaf, N., Mehrabadi, A., Tavakoli, O.: Practical strategies to improve harvestable biomass energy yield in microalgal culture: a review. Biomass Bioenerg. **145**, 105941 (2021). https://doi.org/10.1016/j.biombioe.2020.105941
13. Dalu, T., Wasserman, R.J., Magoro, M.L., Froneman, P.W., Weyl, O.L.F.: River nutrient water and sediment measurements inform on nutrient retention, with implications for eutrophication. Sci. Total Environ. **684**, 296–302 (2019)
14. Fallahi, A., Rezvani, F., Asgharnejad, H., Khorshidi, E., Hajinajaf, N., Higgins, B.: Interactions of microalgae-bacteria consortia for nutrient removal from wastewater: a review. Chemosphere 129878 (2021).
15. Fallah, S., Mamaghani, H.R., Yegani, R., Hajinajaf, N., Pourabbas, B.: Use of graphene substrates for wastewater treatment of textile industries. Adv. Compos. Hybrid Mater. **3**(2), 187–193 (2020)
16. Rabbani, Y., Shariaty-Niassar, M., Ebrahimi, S.A.S. The effect of superhydrophobicity of prickly shape carbonyl iron particles on the oil-water adsorption. *Ceram. Int.* (2021).
17. Asgharnejad, H., Khorshidi Nazloo, E., Madani Larijani, M., Hajinajaf, N., Rashidi, H. Comprehensive review of water management and wastewater treatment in food processing industries in the framework of water-food-environment nexus. *Compr. Rev. Food Sci. Food Saf.*
18. Wang, Q., Higgins, B.T.: Biomass production and Nitrification in an algal-bacterial wastewater treatment system. In *2020 ASABE Annual International Virtual Meeting* p. 1 (2020).
19. Lembi, C.A., Waaland, J.R.: The role of microalgae in liquid waste treatment and reclamation, pp. 251–281. Algae Hum. Aff. Cambridge Univ. Press. Cambridge, UK (1988)
20. Franchino, M., Comino, E., Bona, F., Riggio, V.A.: Growth of three microalgae strains and nutrient removal from an agro-zootechnical digestate. Chemosphere **92**(6), 738–744 (2013)
21. Hultberg, M., Olsson, L.-E., Birgersson, G., Gustafsson, S., Sievertsson, B.: Microalgal growth in municipal wastewater treated in an anaerobic moving bed biofilm reactor. Bioresour. Technol. **207**, 19–23 (2016)
22. Dineshkumar, R., Subramanian, J., Sampathkumar, P.: Prospective of chlorella vulgaris to augment growth and yield parameters along with superior seed qualities in black gram, Vigna mungo (L.). Waste and Biomass Valorization **11**(4), 1279–1287 (2020)
23. Rawat, I., Kumar, R.R., Mutanda, T., Bux, F.: Dual role of microalgae: Phycoremediation of domestic wastewater and biomass production for sustainable biofuels production. Appl. Energy **88**(10), 3411–3424 (2011). https://doi.org/10.1016/J.APENERGY.2010.11.025
24. Hajinajaf, N., Rabbani, Y., Mehrabadi, A., Tavakoli, O.: Experimental and modeling assessment of large-scale cultivation of microalgae Nannochloropsis sp. PTCC 6016 to reach high efficiency lipid extraction. Int. J. Environ. Sci. Technol. (2022). https://doi.org/10.1007/s13762-021-03760-x
25. Fallahi, A., Hajinajaf, N., Tavakoli, O., Mehrabadi, A.: Effects of simultaneous CO2 addition and biomass recycling on growth characteristics of microalgal mixed culture. J. Chem. Technol. Biotechnol. (2021). https://doi.org/10.1002/jctb.6896
26. Azizi, S., et al.: Effect of different light-dark cycles on the membrane fouling, EPS and SMP production in a novel reciprocal membrane photobioreactor (RMPBR) by C. vulgaris species. J. Water Process Eng. **43**, 102256 (2021)
27. Hashemi, A., Shariati, F.P., Sohani, E., Azizi, S., Hosseinifar, S.Z., Amrei, H.D.: CO2 biofixation by Synechococcus elongatus from the power plant flue gas under various light–dark cycles. Clean Technol. Environ. Policy **22**(8), 1735–1743 (2020)
28. Liu, X., et al.: Growth of Chlorella vulgaris and nutrient removal in the wastewater in response to intermittent carbon dioxide. Chemosphere **186**, 977–985 (2017). https://doi.org/10.1016/J.CHEMOSPHERE.2017.07.160
29. Anjos, M., Fernandes, B.D., Vicente, A.A., Teixeira, J.A., Dragone, G.: Optimization of CO2 bio-mitigation by Chlorella vulgaris. Bioresour. Technol. **139**, 149–154 (2013)
30. Mortezaeikia, V., Yegani, R., Tavakoli, O.: Membrane-sparger vs. membrane contactor as a photobioreactors for carbon dioxide biofixation of Synechococcus elongatus in batch and semi-continuous mode. J. CO2 Util. **16**, 23–31 (2016)
31. Gonçalves, A.L., Simões, M., Pires, J.C.M.: The effect of light supply on microalgal growth, CO2 uptake and nutrient removal from wastewater. Energy Convers. Manag. **85**, 530–536 (2014)
32. Carvalho, A.P., Meireles, L.A., Malcata, F.X.: Microalgal reactors: a review of enclosed system designs and performances. Biotechnol. Prog. **22**(6), 1490–1506 (2006)
33. Ho, S.-H., Chen, C.-Y., Lee, D.-J., Chang, J.-S.: Perspectives on microalgal CO2-emission mitigation systems—a review. Biotechnol. Adv. **29**(2), 189–198 (2011). https://doi.org/10.1016/J.BIOTECHADV.2010.11.001

34. Moheimani, N.R.: Inorganic carbon and pH effect on growth and lipid productivity of Tetraselmis suecica and Chlorella sp (Chlorophyta) grown outdoors in bag photobioreactors. J. Appl. Phycol. **25**(2), 387–398 (2013)
35. García-Cubero, R., Moreno-Fernández, J., García-González, M.: Potential of Chlorella vulgaris to abate flue gas. Waste and Biomass Valorization **9**(11), 2015–2019 (2018)
36. Cheng, L., Zhang, L., Chen, H., Gao, C.: Carbon dioxide removal from air by microalgae cultured in a membrane-photobioreactor. Sep. Purif. Technol. **50**(3), 324–329 (2006). https://doi.org/10.1016/J.SEPPUR.2005.12.006
37. Ayatollahi, S.Z., Esmaeilzadeh, F., Mowla, D.: Integrated CO2 capture, nutrients removal and biodiesel production using Chlorella vulgaris. J. Environ. Chem. Eng. **9**(2), 104763 (2020). https://doi.org/10.1016/j.jece.2020.104763
38. Park, J., et al.: Comparative evaluation of CO2 fixation of microalgae strains at various CO2 aeration conditions. Waste Biomass Valorization **12**(6), 2999–3007 (2020). https://doi.org/10.1007/s12649-020-01226-8
39. Chiu, S.-Y., et al.: Microalgal biomass production and on-site bioremediation of carbon dioxide, nitrogen oxide and sulfur dioxide from flue gas using Chlorella sp. cultures. Bioresour. Technol. **102**(19), 9135–9142 (2011)
40. Zhao, Y., Shen, Y., Ma, G., Hao, R.: Adsorption separation of carbon dioxide from flue gas by a molecularly imprinted adsorbent. Environ. Sci. Technol. **48**(3), 1601–1608 (2014)
41. Richmond, A., Hu, Q.: Handbook of microalgal culture. Wiley Online Library (2013)
42. Cheng, J., Huang, Y., Feng, J., Sun, J., Zhou, J., Cen, K.: Improving CO2 fixation efficiency by optimizing Chlorella PY-ZU1 culture conditions in sequential bioreactors. Bioresour. Technol. **144**, 321–327 (2013)
43. Fallahi, A., Hajinajaf, N., Tavakoli, O., Sarrafzadeh, M.H.: Cultivation of mixed microalgae using municipal wastewater: biomass productivity, nutrient removal, and biochemical content. Iran. J. Biotechnol. **18**(4), 88–97 (2020)
44. Thomas, D.M., Mechery, J., Paulose, S.V.: Carbon dioxide capture strategies from flue gas using microalgae: a review. Environ. Sci. Pollut. Res. **23**(17), 16926–16940 (2016)
45. Lee, M.J., Chen, J.T.: Fluid property predictions with the aid of neural networks. Ind. Eng. Chem. Res. **32**(5), 995–997 (1993)
46. Hoskins, J.C., Himmelblau, D.M.: Artificial neural network models of knowledge representation in chemical engineering. Comput. Chem. Eng. **12**(9–10), 881–890 (1988)
47. Engelbrecht, A.P.: Computational intelligence: an introduction. John Wiley & Sons (2007)
48. Hagan, M.T., Menhaj, M.B.: Training feedforward networks with the Marquardt algorithm. IEEE Trans. Neural Networks **5**(6), 989–993 (1994)
49. Rabbani, Y., Shirvani, M., Hashemabadi, S.H., Keshavarz, M.: Application of artificial neural networks and support vector regression modeling in prediction of magnetorheological fluid rheometery. Colloids Surfaces A Physicochem. Eng. Asp. **520**, 268–278 (2017). https://doi.org/10.1016/J.COLSURFA.2017.01.081
50. J. R. Benemann, "Biofixation of CO2 and greenhouse gas abatement with microalgae - Technology roadmap," *Final Rep. to US Dep. Energy. Natl. Energy Technol. Lab.*, vol. 7010000926, pp. 1–29, 2003, [Online]. Available: http://www.ieaghg.org/docs/01roadmp.pdf.
51. Le Gouic, B., Marec, H., Pruvost, J., Cornet, J.F.: Investigation of growth limitation by CO2 mass transfer and inorganic carbon source for the microalga Chlorella vulgaris in a dedicated photobioreactor. Chem. Eng. Sci. **233**, 116388 (2021). https://doi.org/10.1016/j.ces.2020.116388
52. Ryu, H.J., Oh, K.K., Kim, Y.S.: Optimization of the influential factors for the improvement of CO2 utilization efficiency and CO2 mass transfer rate. J. Ind. Eng. Chem. **15**(4), 471–475 (2009). https://doi.org/10.1016/J.JIEC.2008.12.012
53. Singh, B.P.: Biofuel crops: production, physiology and genetics. CABI (2013)
54. He, Q., Yang, H., Hu, C.: Optimizing light regimes on growth and lipid accumulation in Ankistrodesmus fusiformis H1 for biodiesel production. Bioresour. Technol. **198**, 876–883 (2015)
55. Lam, M.K., Lee, K.T.: Effect of carbon source towards the growth of Chlorella vulgaris for CO2 bio-mitigation and biodiesel production. Int. J. Greenh. Gas Control **14**, 169–176 (2013). https://doi.org/10.1016/J.IJGGC.2013.01.016
56. Yang, Y., Gao, K.: Effects of CO 2 concentrations on the freshwater microalgae, Chlamydomonas reinhardtii, Chlorella pyrenoidosa and Scenedesmus obliquus (Chlorophyta). J. Appl. Phycol. **15**(5), 379–389 (2003)
57. Tang, D., Han, W., Li, P., Miao, X., Zhong, J.: CO2 biofixation and fatty acid composition of Scenedesmus obliquus and Chlorella pyrenoidosa in response to different CO2 levels. Bioresour. Technol. **102**(3), 3071–3076 (2011). https://doi.org/10.1016/J.BIORTECH.2010.10.047
58. Sutherland, D.L., Howard-Williams, C., Turnbull, M.H., Broady, P.A., Craggs, R.J.: The effects of CO2 addition along a pH gradient on wastewater microalgal photo-physiology, biomass production and nutrient removal. Water Res. **70**, 9–26 (2015). https://doi.org/10.1016/J.WATRES.2014.10.064
59. Middelburg, J.J.: Biogeochemical processes and inorganic carbon dynamics. In: Middelburg, Jack J. (ed.) Marine carbon biogeochemistry, pp. 77–105. Springer, Cham (2019)
60. Griffiths, M.J., Garcin, C., van Hille, R.P., Harrison, S.T.L.: Interference by pigment in the estimation of microalgal biomass concentration by optical density. J. Microbiol. Methods **85**(2), 119–123 (2011)
61. Barahoei, M., Hatamipour, M.S., Afsharzadeh, S.: CO2 capturing by chlorella vulgaris in a bubble column photo-bioreactor; effect of bubble size on CO2 removal and growth rate. J. CO2 Util. **37**, 9–19 (2020)
62. Hariz, H.B., Takriff, M.S., Ba-Abbad, M.M., Yasin, N.H.M., Hakim, N.I.N.M.: CO 2 fixation capability of Chlorella sp. and its use in treating agricultural wastewater. J. Appl. Phycol. **30**(6), 3017–3027 (2018)
63. Li, F.-F., et al.: Microalgae capture of CO2 from actual flue gas discharged from a combustion chamber. Ind. Eng. Chem. Res. **50**(10), 6496–6502 (2011)
64. Chiu, S.-Y., Kao, C.-Y., Chen, C.-H., Kuan, T.-C., Ong, S.-C., Lin, C.-S.: Reduction of CO2 by a high-density culture of Chlorella sp. in a semicontinuous photobioreactor. Bioresour. Technol. **99**(9), 3389–3396 (2008). https://doi.org/10.1016/J.BIORTECH.2007.08.013
65. Ramanan, R., Kannan, K., Deshkar, A., Yadav, R., Chakrabarti, T.: Enhanced algal CO2 sequestration through calcite deposition by Chlorella sp. and Spirulina platensis in a mini-raceway pond. Bioresour. Technol. **101**(8), 2616–2622 (2010)
66. Sydney, E.B., et al.: Potential carbon dioxide fixation by industrially important microalgae. Bioresour. Technol. **101**(15), 5892–5896 (2010). https://doi.org/10.1016/J.BIORTECH.2010.02.088
67. Chiu, S.-Y., Tsai, M.-T., Kao, C.-Y., Ong, S.-C., Lin, C.-S.: The air-lift photobioreactors with flow patterning for high-density cultures of microalgae and carbon dioxide removal. Eng. Life Sci. **9**(3), 254–260 (2009). https://doi.org/10.1002/elsc.200800113
68. Fan, L.-H., Zhang, Y.-T., Zhang, L., Chen, H.-L.: Evaluation of a membrane-sparged helical tubular photobioreactor for carbon dioxide biofixation by Chlorella vulgaris. J. Memb. Sci. **325**(1), 336–345 (2008). https://doi.org/10.1016/J.MEMSCI.2008.07.044

69. Ding, Y.-D., Zhao, S., Liao, Q., Chen, R., Huang, Y., Zhu, X.: Effect of CO2 bubbles behaviors on microalgal cells distribution and growth in bubble column photobioreactor. Int. J. Hydrogen Energy **41**(8), 4879–4887 (2016). https://doi.org/10.1016/J.IJHYDENE.2015.11.050
70. Castro, M.L.Y., Ballesteros, F.C.: Nutrient removal and biomass production by immobilized chlorella vulgaris. In *Frontiers in water-energy-nexus—nature-based solutions, advanced technologies and best practices for environmental sustainability*, Springer, pp. 187–190 (2020).
71. Bohutskyi, P., et al.: Bioprospecting of microalgae for integrated biomass production and phytoremediation of unsterilized wastewater and anaerobic digestion centrate. Appl. Microbiol. Biotechnol. **99**(14), 6139–6154 (2015)
72. Shanshan, M., Haifeng, L., Yuanhui, Z., Baoming, L., Taili, D., Dongming, Z.: Nitrogen and biomass recovery from low carbon to nitrogen ratio wastewater by combing air stripping and microalgae cultivation. J. Residuals Sci. Technol. **13**(4), S23–S31 (2016)
73. Vymazal, J.: Algae and element cycling in wetlands. Lewis Publishers Inc. (1995)
74. Madigan, M.T., Martinko, J.M., Parker, J.: Brock biology of microorganisms (Vol. 11). Pearson, NY (2017)
75. Caporgno, M.P., et al.: Microalgae cultivation in urban wastewater: nutrient removal and biomass production for biodiesel and methane. Algal Res. **10**, 232–239 (2015). https://doi.org/10.1016/J.ALGAL.2015.05.011
76. Chiang, C.-L., Lee, C.-M., Chen, P.-C.: Utilization of the cyanobacteria Anabaena sp. CH1 in biological carbon dioxide mitigation processes. Bioresour. Technol. **102**(9), 5400–5405 (2011). https://doi.org/10.1016/J.BIORTECH.2010.10.089
77. Fernández, F.G.A., Camacho, F.G., Chisti, Y. Photobioreactors: light regime, mass transfer, and scaleup. In *Progress in industrial microbiology*, vol. 35, Elsevier, pp. 231–247 (1999).
78. Shamoun, B., El Beshbeeshy, M., Bonazza, R.: Light extinction technique for void fraction measurements in bubbly flow. Exp. Fluids **26**(1), 16–26 (1999)
79. Khichi, S.S., Anis, A., Ghosh, S.: Mathematical modeling of light energy flux balance in flat panel photobioreactor for Botryococcus braunii growth, CO2 biofixation and lipid production under varying light regimes. Biochem. Eng. J. **134**, 44–56 (2018)
80. Naderi, G., Znad, H., Tade, M.O.: Investigating and modelling of light intensity distribution inside algal photobioreactor. Chem. Eng. Process. Process Intensif. **122**, 530–537 (2017)
81. Kumar, K., Sirasale, A., Das, D.: Use of image analysis tool for the development of light distribution pattern inside the photobioreactor for the algal cultivation. Bioresour. Technol. **143**, 88–95 (2013)

Authors and Affiliations

Nima Hajinajaf[1] · Alireza Fallahi[1] · Yahya Rabbani[1] · Omid Tavakoli[1] · Mohammad-Hossein Sarrafzadeh[1]

✉ Nima Hajinajaf
nimahajinajaf@gmail.com

✉ Omid Tavakoli
otavakoli@ut.ac.ir

[1] School of Chemical Engineering, College of Engineering, University of Tehran, Tehran 14176, Iran